FPL

L-2015-199
10 CFR 52.3

July 15, 2015

U.S. Nuclear Regulatory Commission
Attn: Document Control Desk
Washington, D.C. 20555-0001

Re: Florida Power & Light Company
Proposed Turkey Point Units 6 and 7
Docket Nos. 52-040 and 52-041
Response and Revised Response to NRC Request for Additional Information Letter No. 082 (eRAI 7811) SRP Section 02.05.04 – Stability of Subsurface Materials and Foundations

References:

1. NRC Letter to FPL dated February 18, 2015 Request for Additional Information Letter No. 082 Related to SRP Section 02.05.04 – Stability of Subsurface Materials and Foundations for the Turkey Point Nuclear Plant Units 6 and 7 Combined License Application
2. FPL Letter L-2015-131 to NRC dated April 29, 2015, Response to NRC Request for Additional Information Letter No. 082 (eRAI 7811) SRP Section 02.05.04 – Stability of Subsurface Materials and Foundations

Florida Power & Light Company (FPL) provides, as an attachment to this letter, its response to the Nuclear Regulatory Commission's (NRC) request for additional information (RAI) 02.05.04-26 provided in Reference 1.

Additionally, FPL and NRC Staff have been engaged in interactions with respect to the information submitted in Reference 2.

As a result of these interactions, Florida Power & Light Company (FPL) is providing, as an attachment to this letter, a revised response for the Nuclear Regulatory Commission's (NRC) Request for Additional Information (RAI) RAI 02.05.04-27 provided in Reference 2.

The attachments identify changes that will be made in a future revision of the Turkey Point Units 6 and 7 Combined License Application (if applicable).

D097
NRO

I declare under penalty of perjury that the foregoing is true and correct.

Executed on July 15, 2015

Sincerely,

William Maher
Senior Licensing Director – New Nuclear Projects

WDM/RFB

Attachment 1: FPL Response to NRC RAI No. 02.05.04-26 (eRAI 7811)
Attachment 2: FPL Revised Response to NRC RAI No. 02.05.04-27 (eRAI 7811)

cc:
PTN 6 & 7 Project Manager, AP1000 Projects Branch 1, USNRC DNRL/NRO
Regional Administrator, Region II, USNRC
Senior Resident Inspector, USNRC, Turkey Point Plant 3 & 4

NRC RAI Letter No. PTN-RAI-LTR-082

SRP Section: 02.05.04 - Stability of Subsurface Materials and Foundations

Question from Geosciences and Geotechnical Engineering Branch 1 (RGS1)

NRC RAI Number: 02.05.04-26 (eRAI 7811)

In FSAR Subsection 2.5.4.4.5.5, the applicant commits to performing microgravity surveys on the excavation surfaces of the proposed Units 6 and 7 to detect the presence, or verify the absence, of potential water-filled dissolution features (or voids) beneath the power block. Interpretations of the existing gravity survey anomalies discussed in FSAR 2.5.4.4.5.1 include uncertainties related to significant lateral variations in the shallow soil layers that will be removed prior to construction of Units 6 and 7. FSAR Subsection 2.5.4.4.5.5 states that "The [new] micro- gravity survey will be designed to detect 25-foot diameter spherical voids and cylindrical voids as small as 12 feet in diameter at the base of the 25-foot-thick grout plug at an elevation of approximately –60 feet NAVD 88." If the new gravity data (collected after the excavations are completed) indicate that there might be some gravity anomalies of concern, the applicant plans to drill those areas where such anomalies are observed to understand the source of these anomalies. In accordance with 10 CFR 100.23, please provide the following to assist NRC staff's further review in this area:

1. Clarification and demonstration that only the voids greater than the 25-foot spherical diameter and/or 12-foot cylindrical diameter at an elevation of about –60 feet are critical to the stability of subsurface materials and the integrity of structures, systems, and components (SSCs).
2. If voids smaller than the above mentioned dimensions impact the stability of subsurface materials and are critical to the integrity of SSCs, please provide further information on void size, location and depth in the limestone layers that need to be considered.
3. Additional details on the planned microgravity gravity survey specifically:
    a. Address the size of the areas to be investigated
    b. Will measurements be conducted along profiles or the entire excavated surfaces surveyed
    c. Measurement intervals, and data reduction and processing methodologies to be employed considering the three-dimensionality of the excavations and their impact on the gravity measurements
4. A description of the type of inspection and test program to be followed to reasonably ensure that gravity anomalies resulting from potential underground voids (both within the grouted zones and deeper levels) that are critical to the stability of subsurface materials and the integrity of SSCs are to be appropriately detected, investigated, evaluated and, if necessary, remediated.

FPL RESPONSE:

Summary of Conclusions on Karstic Structures from Geological Perspective:

Before describing the method used to determine void size and the numerical models for stability, it is important to re-emphasize the geological conclusion (FSAR Appendix 2.5AA, summarized below) that large voids and karst features are considered unlikely to be present at the site. The geological evaluation of the site is necessary to confirm if karstic structures are present on site and, if so, to establish the likely size and extent of the karstic structures. In this regard, the following are key points to be considered as outlined in FSAR Appendix 2.5AA and the Response to RAI 02.05.01-37.

- Neither the vegetated depressions nor the zones of secondary porosity are considered to pose a hazard of sinkhole development. The vegetated depressions are surficial solution features formed by a subaerial, epigenic process of dissolution caused by downward seepage of slightly acidic meteoric groundwater. The zones of secondary porosity are microkarst features formed in the subsurface by solution enlargement of touching-vug and moldic porosity within paleomixing zones of fresh groundwater and saltwater. An upper zone of secondary porosity has formed in a zone of touching-vug porosity near the contact of the Miami Limestone and the Key Largo Limestone. A lower zone of secondary porosity has formed in a zone of moldic porosity in the underlying Fort Thompson Formation. Microkarst features are in the order of a few centimeters.
- The process that formed the vegetated depressions at the site and its vicinity is ongoing. However, the stratigraphic interval in which they occur will be completely removed during excavation of the nuclear islands. As discussed below, the structure contour and isopach maps indicate that the surficial vegetated depressions do not persist with depth. In addition, the freshwater/saltwater interface is approximately 6 miles inland from the site, and mean sea level rise trend is low (0.78 foot in 100 years); thus, the carbonate dissolution in a fresh groundwater/saltwater mixing zone by the process of shoreline flow is not likely to develop large underground voids.
- As discussed in the Response to RAI 02.05.01-37, available information related to caves, cover collapse sinkholes, springs, submarine sinkholes, paleo-karst collapses, and sag structures in the site vicinity (and in other areas in southeast Florida) suggests that, while dissolution features are present, most are not currently active. Active dissolution is probably limited at Turkey Point Units 6 & 7, as is the potential for deformation due to collapses within existing (i.e., "paleo") dissolution features. Active dissolution associated with karst conduits at the site, as evident in past submarine groundwater discharges, is also likely to be insignificant. Furthermore, the observed collapse structures at Jewfish Creek/Lake Surprise (17 miles from Turkey Point Units 6 & 7), for example, appears to have occurred in the Pleistocene (coincident with sea level lowstands) and thus is not a particularly relevant analog for potentially active (or possible future) surface collapse at (or near) the site. No structural damage or differential settlement has been reported on the bridge that was constructed on the Jewfish Creek/Lake Surprise site that was described in the Response to RAI 02.05.01-

37. Although substantial in scale and extent, the seismic sag structures described by Cunningham and Walker (FSAR Reference 2.5.1-958) similarly provide no evidence for post-Pliocene deformation. It seems likely then that comparable collapses in similar features, if present below Turkey Point Units 6 & 7, have already occurred (and are now stabilized).

- Finally, structure contour and isopach maps for the Key Largo Limestone and Fort Thompson Formation and cross-sections prepared with data from the site geotechnical subsurface investigation do not suggest the existence of large underground caverns or sinkholes. Specifically, the following conclusions are obtained (as provided in the Response to RAI 02.05.04-01) for the sizes of potential voids and/or voids filled with soft sediments:

  "...The evaluation of all data (MACTEC, Reference 6; RIZZO, Reference 3) indicate that outside the vegetated depressions and drainages (in vertical borings), a total of 20.1 feet of interpreted tool drops (due to voids and/or voids filled with soft sediments) are observed, in a total of 7918.4 feet cored, for a 0.3 percent of the total cored in 93 borings. Individual drops in the vertical borings range from 0.4 feet to 4 feet (1.5 feet max within the Unit 6 & 7 building footprints). Results from the site investigations (MACTEC, Reference 6; RIZZO, Reference 3), show that interpreted tool drops are found more often under the vegetated depressions and drainages. In the three inclined borings, a total of 15.2 feet of tool drops are observed, in a total of 356.4 feet cored, for a 4.3 percent of the total cored length. Individual drops in the inclined borings range from 0.3 feet to 2.5 feet. Boring locations with interpreted tool drops, among all sampling locations, are shown in Figure 1.

  The maximum length of interpreted tool drop (due to voids and/or voids filled with soft sediments) is limited to 1.5 feet within the Unit 6 & 7 building footprints, and the frequency of encountering an interpreted tool drop is less than 0.5 percent site-wide. These statistics are based on the drilling conducted during both, the initial and supplemental site investigations (MACTEC, Reference 6; RIZZO, Reference 3)..."

<u>The following methodology is employed to respond to RAI 02.05.04-26:</u>

Instead of developing the critical void size via microgravity methods, which can only detect large voids at depth, the subsurface grouting program, which was planned only for dewatering purposes, will be considered in the determination of constrained void sizes. Part 4 of this response provides an Inspection, Tests, Analyses, and Acceptance Criteria (ITAAC) to ensure that the zone between El. –35 feet and El. –60 feet within the diaphragm walls will be grouted according to the closure criteria that will be developed as part of the grout test program. This grouting will ensure that any potential voids in this zone are filled. In addition, for the zone between El. –60 feet and –110 feet within the diaphragm walls, grouting will be performed in every primary grout borehole. Primary grout holes will be spaced less than or equal to 20 feet on center. This

configuration, as shown in Figure 1, is expected to constrain the maximum undetected void size to approximately 20 feet.

Figure 1 Primary Grout Borehole Layout

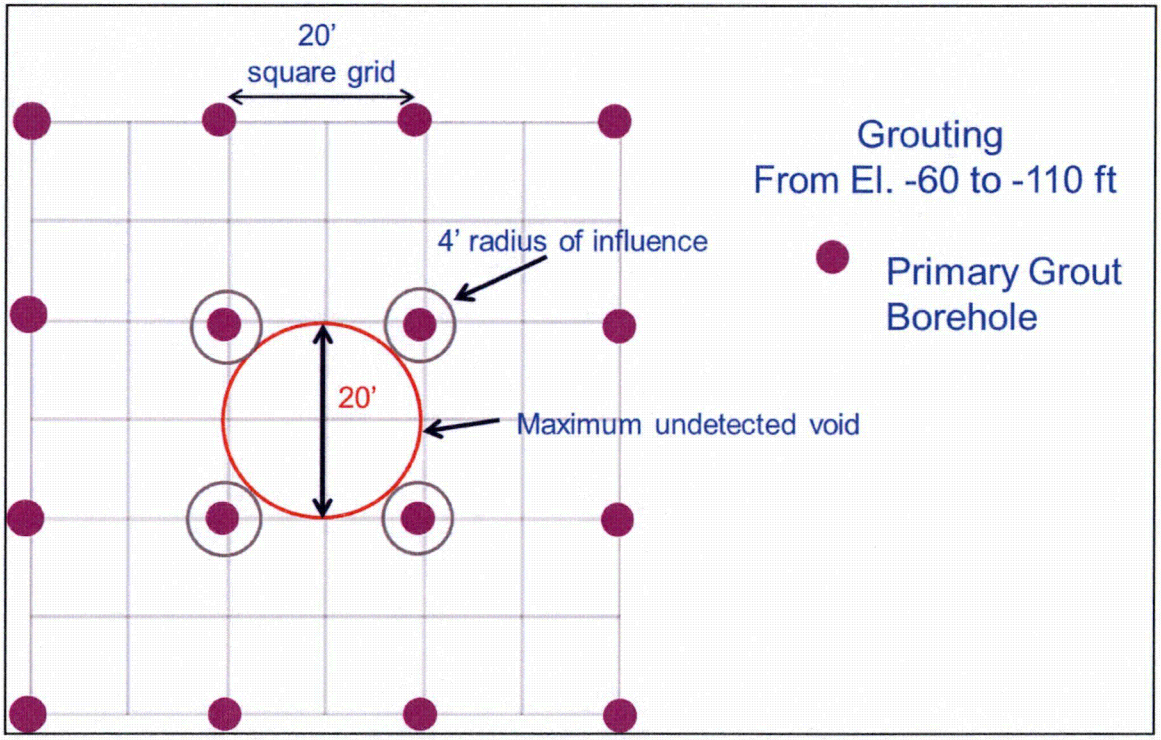

The void size (20-feet) constrained by the grouting program is conservatively much larger than the estimated void sizes present on site, and has been evaluated in static (settlement and bearing capacity) and dynamic (pseudo-dynamic) analyses. ITAAC are also provided to ensure that potential voids in the zone between El. –35 feet and –60 feet are remediated, and the potential voids between El. –60 feet and El. –110 feet are partially remediated (i.e., only primary grout holes).

Part 1)

In response to Part 1, a sensitivity analysis is performed, including static (settlement and bearing capacity) and pseudo-dynamic evaluations, to demonstrate that the void size constrained by the grouting program is not critical to the stability of subsurface materials and the integrity of SSCs.

Void Sizes and Depths Considered

The analysis considers the zone between El. –35 feet and El. –60 feet to be completely grouted and void free. The zone between El. –60 feet and El. –110 feet will be grouted partially at primary grout holes spaced 20 feet apart. This spacing, with a typical grout

radius of influence of 4 feet, corresponds to a sphere shaped void with a maximum 20 feet equivalent diameter (as shown in Figure 1).

A very extreme case of a tunnel (cylindrical) shaped void with a 20-foot diameter circular cross-section is considered where the void extends east-west across the nuclear island with the top of the void just below the grout plug (El. –60 feet). This direction is selected since the maximum seismic overturning moment acts in the east-west direction.

The sensitivity analysis considers extremely unlikely and conservative cases that are only reported to show the safety margin provided by the rock mass; these cases are highly unlikely and are not for design purposes.

Modeling Approach

For the analysis, the 3D finite element model (as presented in the Response to RAI 02.05.04-19) is updated for the void case presented above. Best estimate material properties (FD1 properties for rock layers) are used for this analysis, as described in the Response to RAI 02.05.04-19.

The void is assumed to be water-filled, and is therefore modeled with the same pore pressures as the surrounding rock.

The model considers a construction sequence that includes the following activities:

- Initial gravity loading (without the void),
- Gravity loading (with the void),
- Dewatering,
- Excavation and fill placement,
- Loading, and
- Rewatering.

The void is not considered in the initial gravity loading phase because it would have developed over time; further, inserting the void in the second phase allows for an evaluation of any points reaching Mohr-Coulomb failure due to the presence of the void independent from the other construction activities.

Nuclear Regulatory Commission (NRC) RG 1.132 Appendix D states that, "*Where soils are very thick, the maximum required depth for engineering purposes, denoted* d_{max}, *may be taken as the depth at which the change in the vertical stress during or after construction for the combined foundation loadings is less than 10% of the effective in situ overburden stress.*" The analysis depth of El. –450 feet, which is greater than 2B (B = the least dimension of the foundation), was assumed to be adequate to meet the aforementioned criterion. In situ initial overburden effective vertical stress at the bottom of the model is compared to the effective vertical stress at the bottom of the model for each phase. The changes in effective vertical stresses are less than 10 percent of the effective in situ stress for each phase, demonstrating that the model depth is appropriate.

As discussed in the Response to RAI 02.05.04-19, the plan dimensions considered in the model are 1724 feet by 1396 feet. The lateral boundary conditions were checked by confirming that the horizontal stresses at the edge of the model are in agreement with horizontal stresses calculated by hand. Effective horizontal stresses are calculated using Equations 1 and 2, below (Reference 1).

$$\sigma'_h = K_0 \times \sigma'_v \qquad \text{Equation 1}$$

Where,

σ'_h = the effective horizontal stress,

σ'_v = the effective vertical stress,

and K_0 = the at rest earth pressure coefficient

$$K_0 = \frac{\nu}{1-\nu} \qquad \text{Equation 2}$$

Where,

ν = Poisson's ratio

Figures 2 and 3 show a comparison of the effective horizontal stresses at the east (effective horizontal stress = σ'_{xx} since the plain strain conditions prevail in xx-direction) and north (effective horizontal stress = σ'_{zz} since the plain strain conditions prevail in zz-direction) boundaries of the model with the horizontal stresses calculated by hand. Model stresses are shown for the initial phase and loading phases. The average differences per layer between the effective horizontal stresses in the initial and loading phases are provided in Table 1. Figures 2 and 3 generally demonstrate good agreement between the effective horizontal stresses at the model boundary and the horizontal stresses calculated by hand, confirming that the model extent is appropriate.

The lateral boundary conditions were also checked in the Response to RAI 02.05.04-19 by demonstrating that the total displacement at the corner of the model is less than 0.1 inches. Additionally, a sensitivity analysis was performed for the best estimate model (presented in the Response to RAI 02.05.04-19), where the model boundaries were extended such that the distance from the buildings to the edge of the model is approximately twice that of the best estimate model. Maximum settlement predicted for the buildings does not vary with the extended boundaries, also confirming that the lateral extent of the best estimate model is adequate.

Figure 2 Effective Horizontal Stresses – East Model Boundary

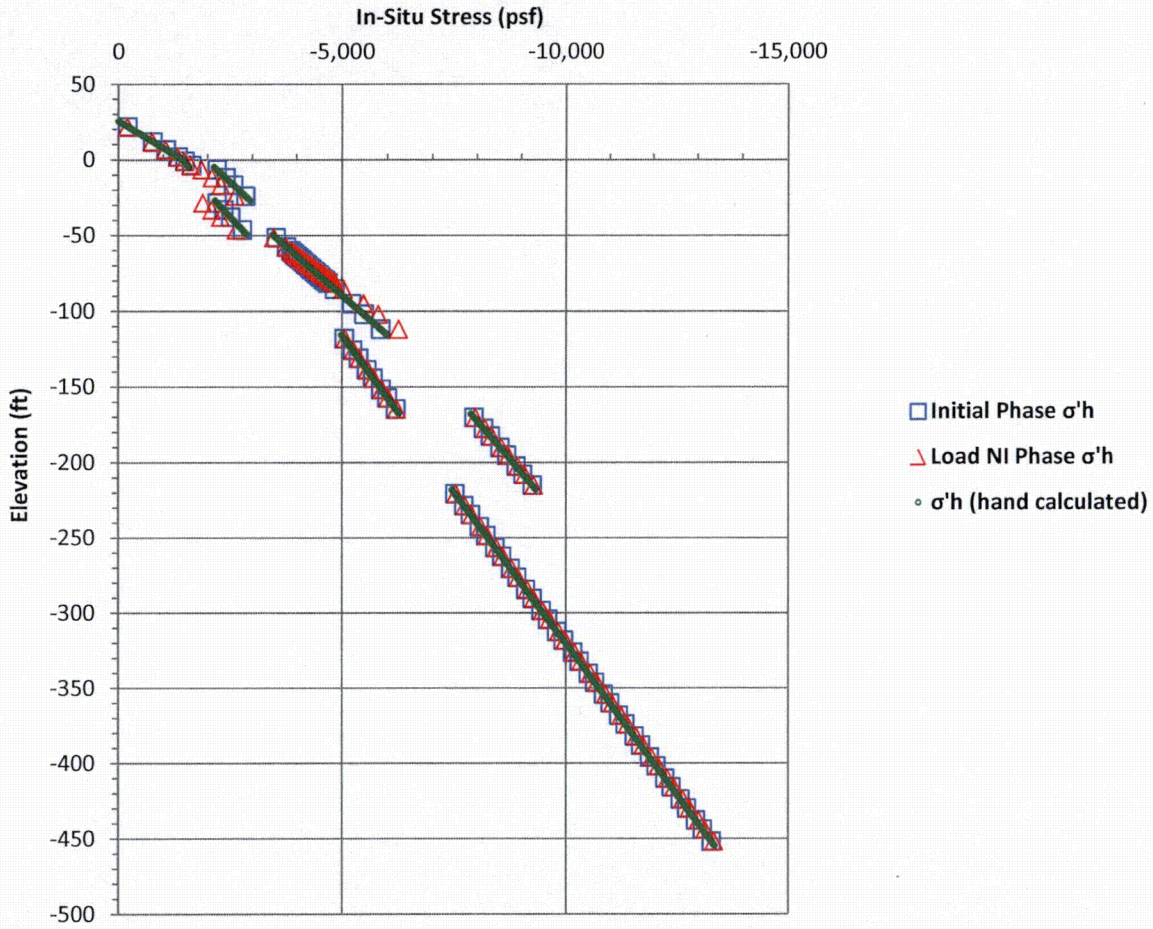

Figure 3 Effective Horizontal Stresses – North Model Boundary

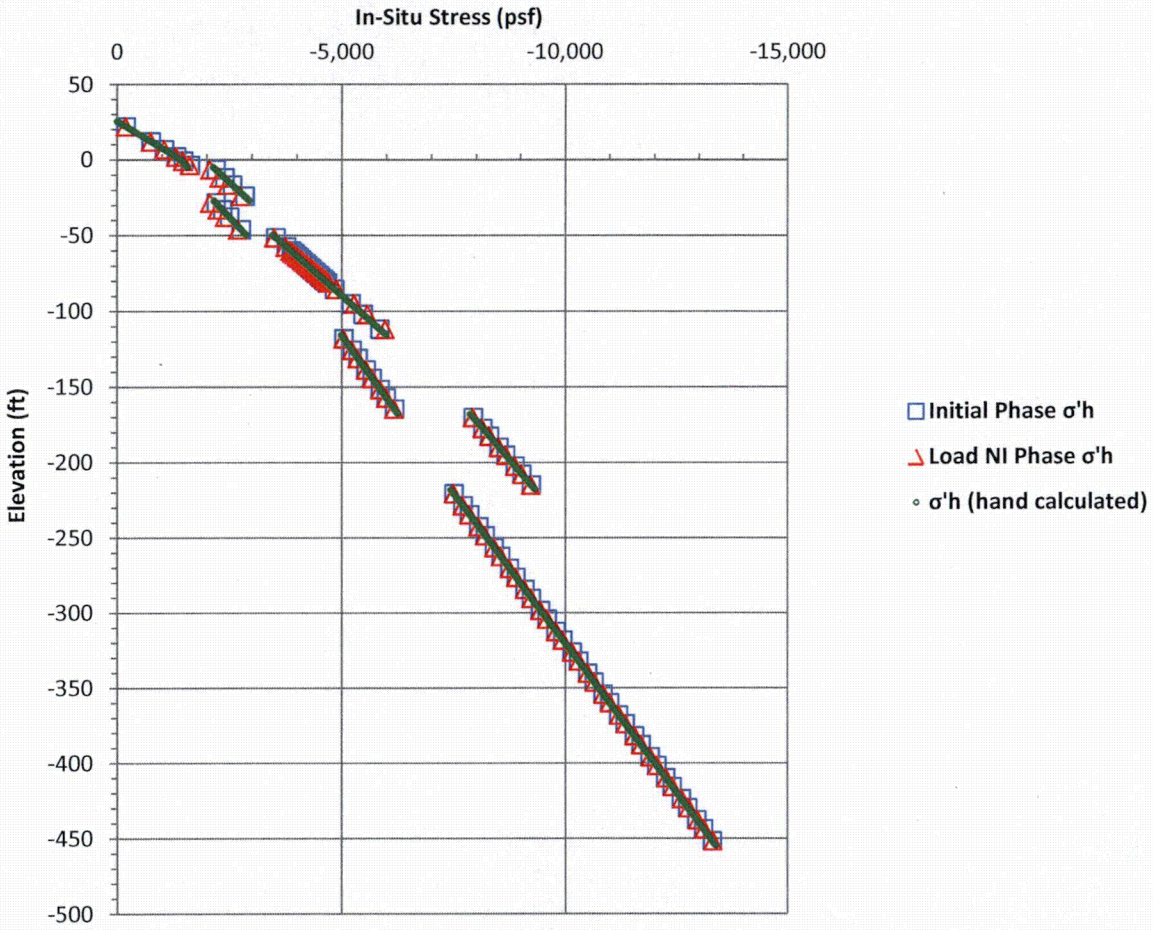

Table 1
Percent Difference between Effective Horizontal Stresses in the Initial and Loading Phases

Formation	North Model Boundary	East Model Boundary
Backfill	1%	1%
Miami Limestone	5%	12%
Key Largo Limestone	4%	10%
Fort Thompson Formation	1%	2%
Upper Tamiami	0%	0%
Lower Tamiami	0%	0%
Peace River	0%	0%

Figures 4 through 6 show the PLAXIS3D model. The 3D mesh is refined to the extent possible in the area surrounding the void. The total number of elements is 103,136.

Figure 4 PLAXIS3D Model

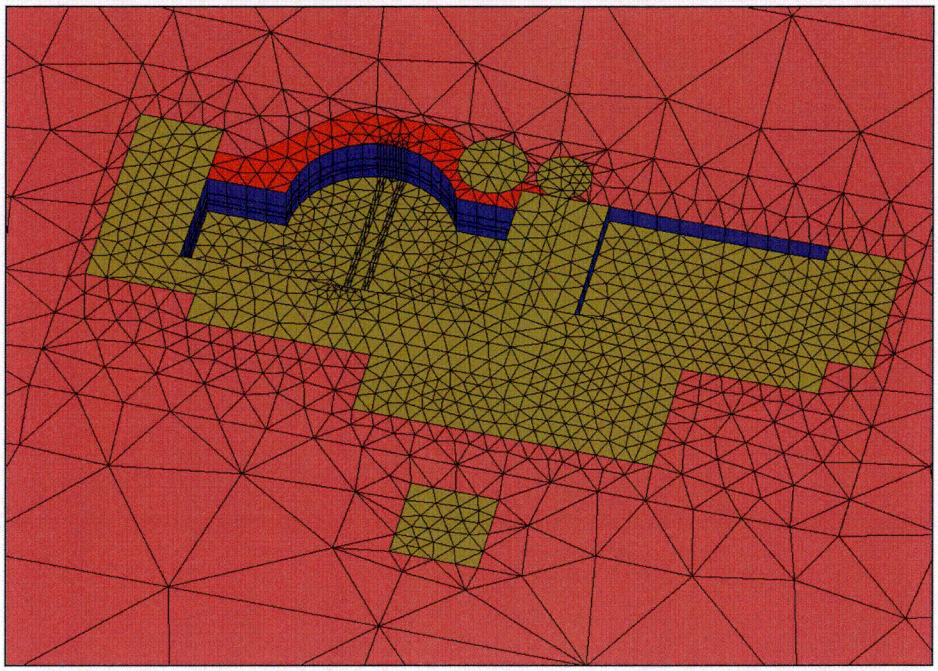

Figure 5 PLAXIS3D Model – Plan View

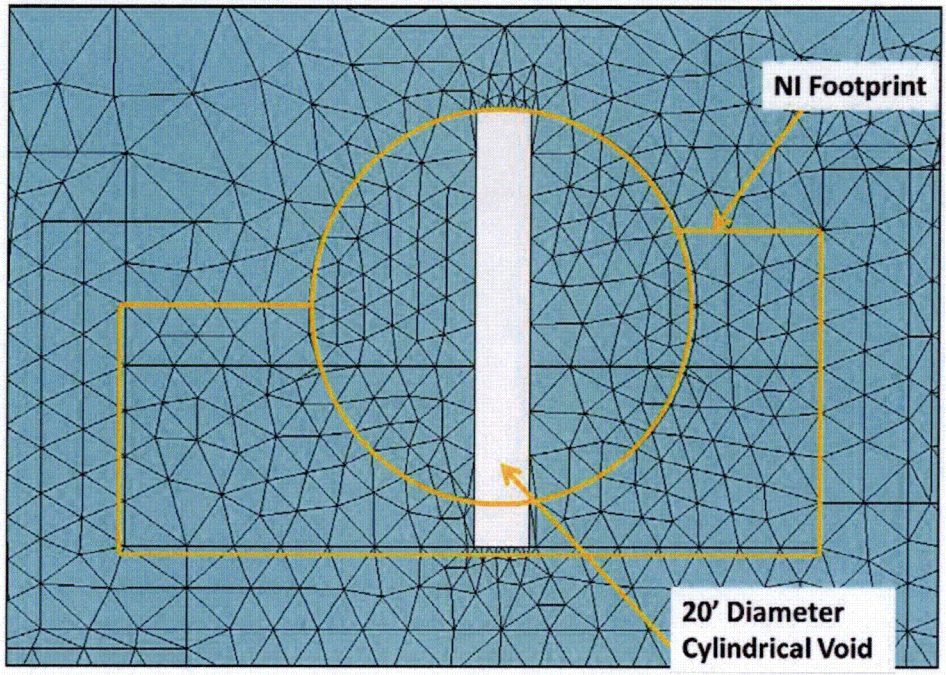

Figure 6 PLAXIS3D Model – Cross-Section

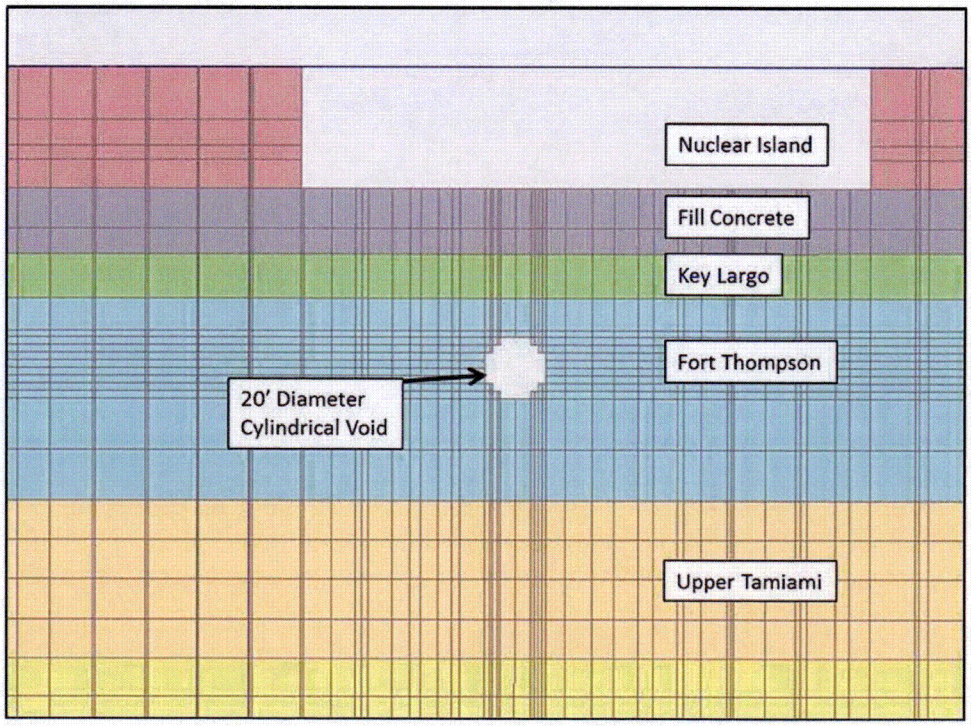

Settlement

Vertical deformation due to loading is evaluated in the PLAXIS3D finite element models to determine the impact of the potential void on the settlement of the nuclear island. Differential settlements are calculated and the results are compared to the DCD requirements.

Bearing Capacity

To determine the impact of the potential void on the bearing capacity, the model is incrementally loaded up to much higher loads than the actual building loads and a load displacement curve is developed. This curve is used to evaluate the bearing capacity.

Concrete Fill Properties

In order to assess potential tension in the concrete, the concrete is assumed to be a Mohr-Coulomb material in the PLAXIS3D model with a friction angle of 0 degrees, cohesion of 108,000 psf, and tensile strength of 21,600 psf, based on Equation 3 (Reference 1), Equation 4 (Reference 2), and a compressive strength of 1500 psi.

$$\boldsymbol{Cohesion} = \frac{\boldsymbol{Compressive\ Strength}}{2} \qquad \textbf{Equation 3}$$

$$\boldsymbol{Tensile\ Strength} \approx \mathbf{0.1} \times \boldsymbol{Compressive\ Strength} \qquad \textbf{Equation 4}$$

Pseudo-Dynamic

To consider the impact of the potential voids on under dynamic conditions, dynamic bearing pressures from the SASSI model are converted to equivalent (approximately) static loads and applied to the PLAXIS 3D model.

The forces from the dynamic bearing pressures are summed up and distributed uniformly over areas of the eastern (maximum uplift) and western half (maximum compression) of the nuclear island. The maximum uplift bearing pressures as obtained from the upper bound, lower bound, and best estimate cases are applied on the east half of the nuclear island, whereas the maximum compressive bearing pressures as obtained from the upper bound, lower bound, and best estimate cases are applied on the west half of the nuclear island, such that the maximum overturning moment is applied on the western edge of the nuclear island.

This approach is very conservative because

- Nodal maximum bearing pressures are used regardless of their time step (note that maximum pressures for each node correspond to different time steps, i.e., they do not happen at the same time).
- Maximum compressive pressures and tensile pressures are applied at the same time to maximize the overturning moment.

Additionally, a case is considered where the load combinations are multiplied by a safety factor of 2. Table 2, below shows the total loads considered (static and pseudo-

dynamic). The sum of the static load and the seismic uplift pressure is positive, if the overall pressure is compressive.

Table 2
Pseudo-Dynamic Loads (ksf)

Building	Multiplier of 1		Multiplier of 2	
	West Half of NI	East Half of NI	West Half of NI	East Half of NI
Shield Building	-16.2	-8.1	-32.3	-4.3
North Auxiliary Building	-9.5	-1.4	-18.9	2.4
South Auxiliary Building	-12.1	-4.0	-24.1	-0.2

Note: Negative sign indicates compressive loads, positive sign indicates uplift loads.

The bearing pressures corresponding to the combination of dead loads and the maximum moment are checked against the bearing capacity of the concrete fill. The ultimate bearing capacity for the concrete fill is estimated to be 1275 psi (184 ksf) using Equation 5 (Reference 3) and a compressive strength of 1500 psi.

$$Ultimate\ Bearing\ Capacity = 0.85 \times f'c \qquad \text{Equation 5}$$

Where,

f'c = compressive strength

Results

All model results presented are for the case with a tunnel (cylindrical) shaped void with a 20-foot diameter circular cross-section. The tunnel (cylindrical) shaped void is considered to be more critical than a smaller 20-foot diameter spherical void, or a distribution of spherical voids.

Soil layers are modeled using Mohr-Coulomb material properties. The Mohr's failure stress circle is controlled by the principal stresses and strength properties (friction angle and cohesion) of the material, as shown by the governing equations below (Reference 1).

$$s = c + \sigma\tan(\varphi) \qquad \text{Equation 6}$$

$$\sigma_1 = \sigma_3 tan^2\left(45° + \frac{\varphi}{2}\right) + 2c\tan\left(45° + \frac{\varphi}{2}\right) \qquad \text{Equation 7}$$

$$\sigma_3 = \sigma_1 tan^2\left(45° - \frac{\varphi}{2}\right) - 2c tan\left(45° - \frac{\varphi}{2}\right) \qquad \text{Equation 8}$$

Where,

s = shear strength

c = cohesion

φ = friction angle

σ_1 = major principal stress

σ_3 = minor principal stress

Results are evaluated in terms of effective vertical stresses, shear stresses, and plastic points (points reaching the Mohr-Coulomb failure envelope). Effective vertical stress and shear stress plots are utilized to identify the high-stress areas (hot spots). In other words, they are used to develop a "feel" for the behavior. The static stability check is actually governed by the following four factors:

1. Accumulation of plastic points indicating a local (e.g., around the void) or global (e.g., bearing capacity) failure.
2. Deformations exceeding DCD limits.
3. Concrete layer experiencing tension failure.
4. Bearing capacity with FS<3.

Effective vertical stresses from the PLAXIS3D model are shown in Figures 7 and 8, below. Negative effective stresses presented in Figures 7 and 8 represent compression, while positive effective stresses represent tension. Larger compressive stresses are observed on the sides of the void indicating the expected deformation of the void under building loads. Effective vertical stresses are highest at the edges of the voids in the models, as anticipated, since the stresses are expected to concentrate around the voids particularly. Some effective stresses are larger in areas of sharp discontinuities, which are artificial products of finite element modeling. Stresses at these locations are not expected to be this high, since the realistic stress distribution is expected to be smoother.

Figure 7 Effective Vertical Stresses from PLAXIS3D (Gravity Loading with the Void)

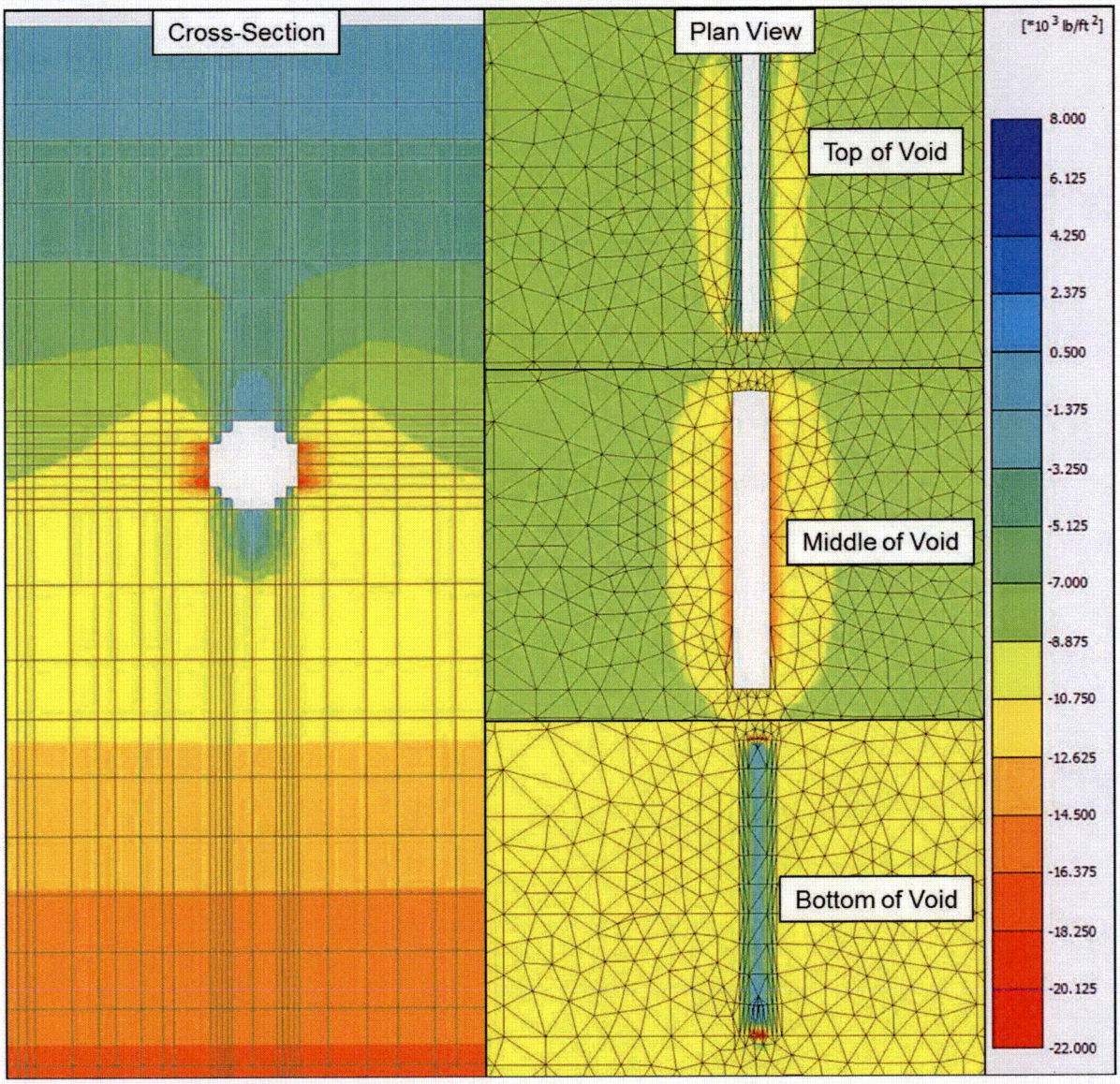

Note: Negative effective stresses represent compression, while positive effective stresses represent tension.

Figure 8 Effective Vertical Stresses from PLAXIS3D (Static Loading Phase)

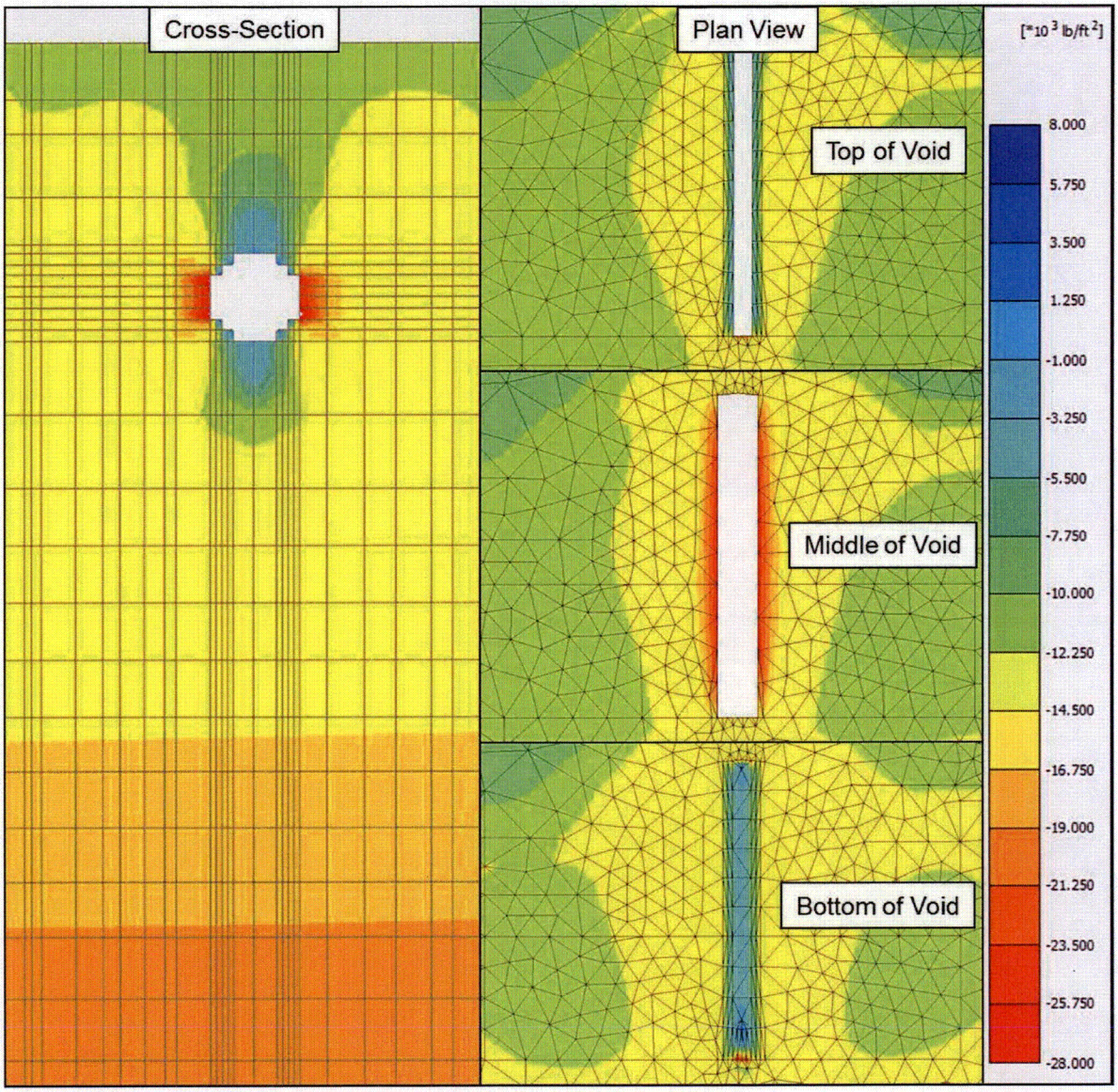

Note: Negative effective stresses represent compression, while positive effective stresses represent tension.

Shear stresses from the PLAXIS3D models are shown in Figures 9 and 10, below. Shear stresses are highest at the edges of the voids, as expected.

Figure 9 Shear Stresses from PLAXIS3D (Gravity Loading with the Void)

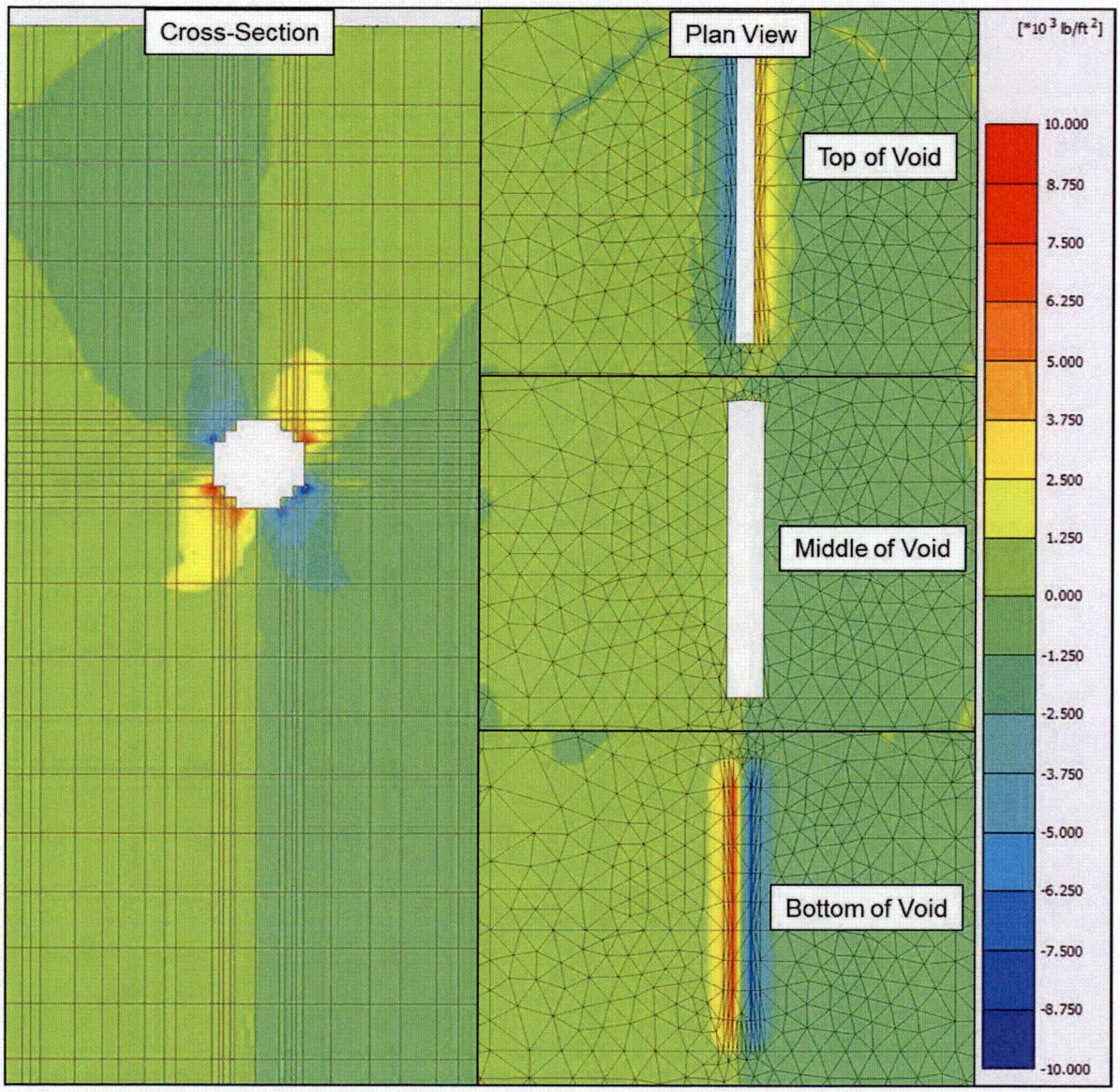

Figure 10 Shear Stresses from PLAXIS3D (Static Loading)

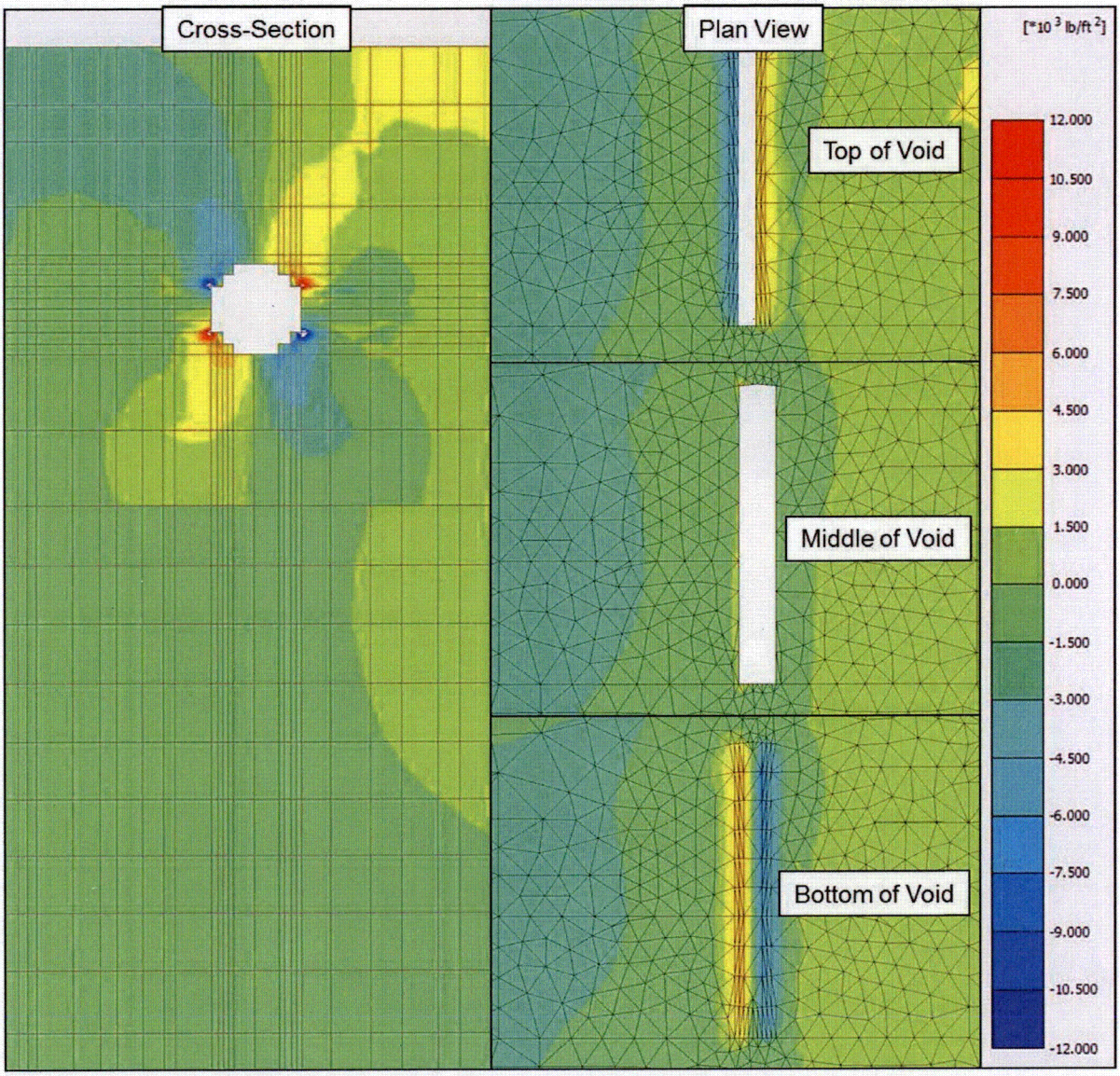

Yield at any point is considered to occur if the stress state reaches the Mohr-Coulomb failure envelope. As shown in Figure 11, there are no plastic points (indicated by red squares) or tension cut-off points (indicated by blue squares) near the void location indicating that the rock mass surrounding the void is not experiencing compressive failure according to Mohr-Coulomb failure envelope or points where the tensile load exceeds the tensile capacity. No tension cut-off points are identified within the concrete fill, i.e., the tension in the concrete fill is less than the tensile capacity of the concrete fill.

Figure 11 Plastic Points PLAXIS3D (Static Loading)

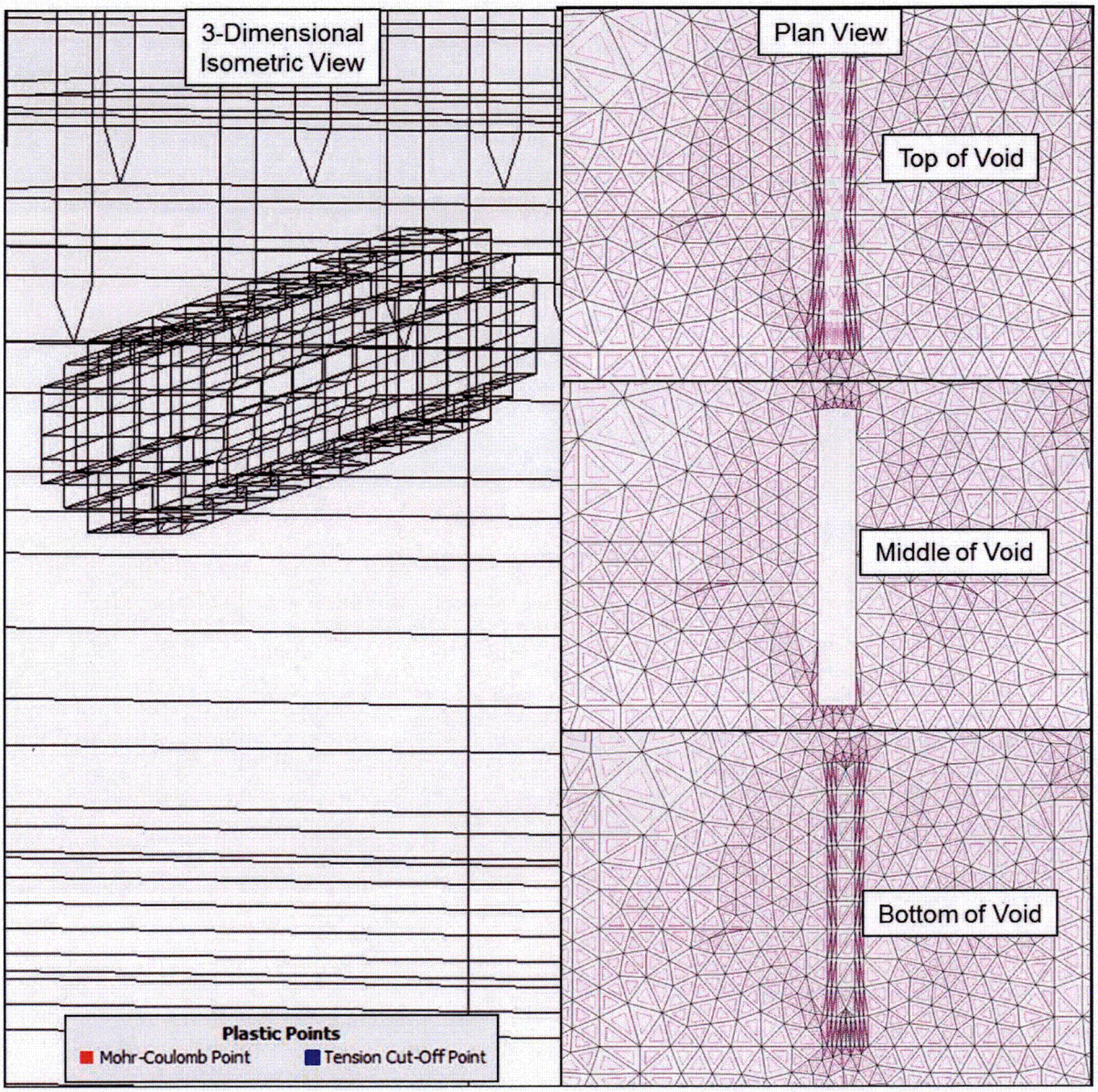

Another useful parameter to consider is the relative shear stress, which is a measure to define how close the stress state is to the Mohr-Coulomb failure envelope. Relative shear stresses are defined in Equation 9 (Reference 4).

$$\tau_{rel} = \frac{\tau_{mob}}{\tau_{max}}$$ Equation 9

Where,

τ_{rel} = relative shear stress,

τ_{mob} = mobilized shear strength (maximum value of shear stress),

τ_{max} = maximum value of shear stress for the case where the Mohr's circle is expanded to touch the Coulomb failure envelope while keeping the center of Mohr's circle constant.

Based on Equation 9, relative shear stresses provide a measure of margin compared to Mohr-Coulomb failure. For example, if the relative shear stress is equal to 1, then that location is marked with a plastic point. If the relative shear stress is much less than 1, the point is not close to the Mohr-Coulomb failure envelope. As shown by Figure 12, the rock surrounding the void indicates relative shear stresses much less than 1.

In conclusion, the presence of a 20-foot wide tunnel as modeled here does not present stability concerns, i.e., no subsurface collapse is anticipated.

Figure 12 Relative Shear Stresses (Static Loading)

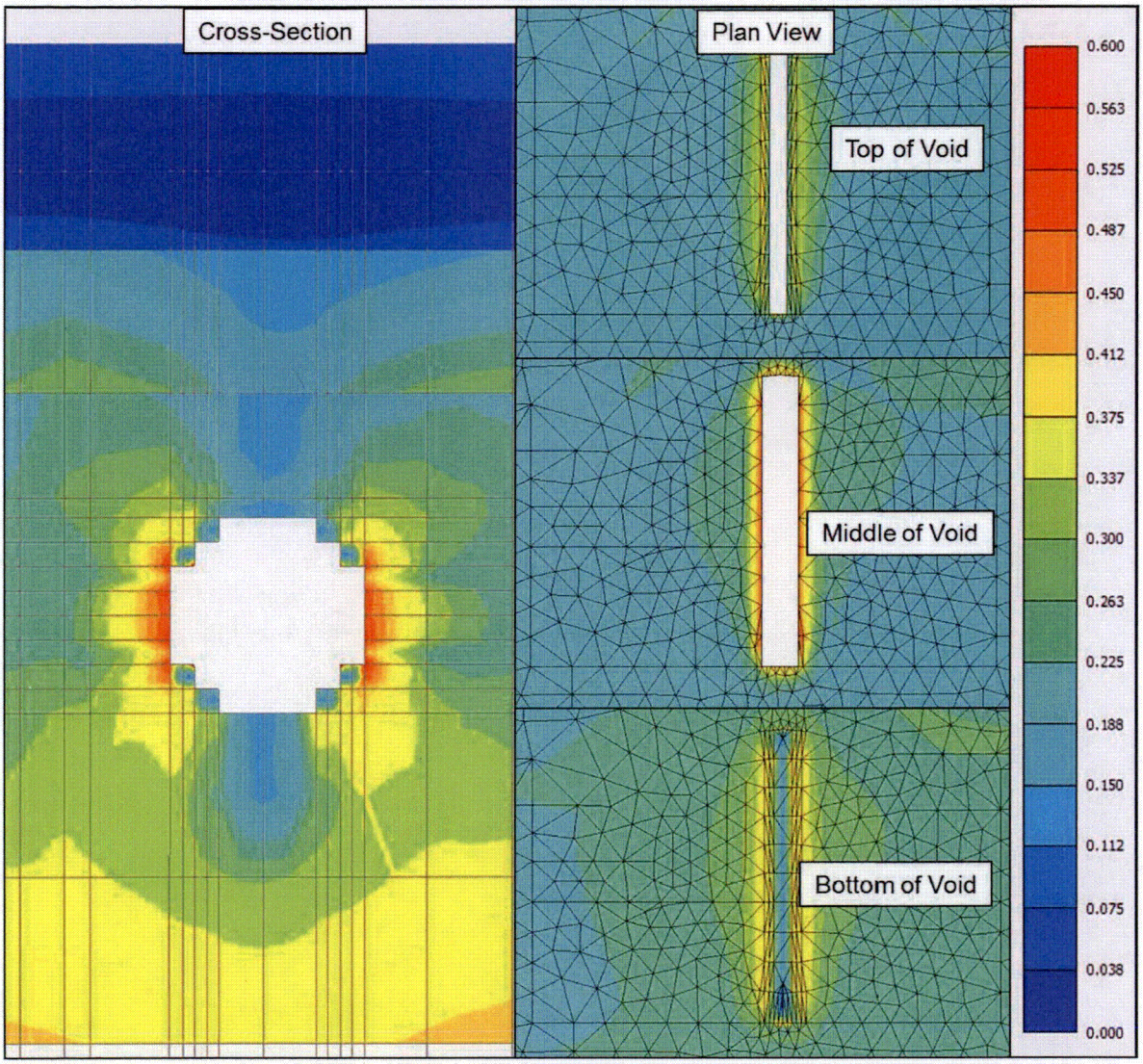

The total and differential settlements from the PLAXIS3D model are presented in Table 3, below. For reference, Table 3 also includes the DCD requirements and the settlements for the model without voids (as presented in the Response to RAI 02.05.04-19). These results show that the presence of the void has no impact on settlement, and that the DCD criteria are still met. The total vertical deformation (loading nuclear island phase) from the PLAXIS3D model is shown in Figure 13, below. Therefore the void cases considered are not critical to the settlement of safety related structures.

Table 3
Total and Differential Settlements Compared to DCD Criteria

	Differential Across Nuclear Island Foundation Mat (inch per 50 feet)	Total for Nuclear Island Foundation Mat (inch)	Differential Between Nuclear Island and Turbine Building[1] (inch)	Differential Between Nuclear Island and Other Buildings[1][2] (inch)
DCD Requirement	0.5	6	3	3
Plaxis 3D (No Void)	0.20	2.53	0.79	1.60
Plaxis 3D (20' Diameter Tunnel Void)	0.20	2.52	0.79	1.61

1. Differential settlement is measured at the center of the nuclear island and the center of adjacent structures.
2. Maximum differential settlement occurs between nuclear island and radwaste buildings.
3. Settlements presented exclude the rewatering phase.
4. Settlements are presented to two decimal places to show that differences in settlement between the Plaxis 3D model (No Void) and Plaxis 3D model (20' Diameter Tunnel Void) are negligible. These negligible differences in settlement are considered to be within the variability of the software, and may be due to the different meshes of the finite element models.

Figure 13 Total Vertical Deformation PLAXIS3D (Static Loading)

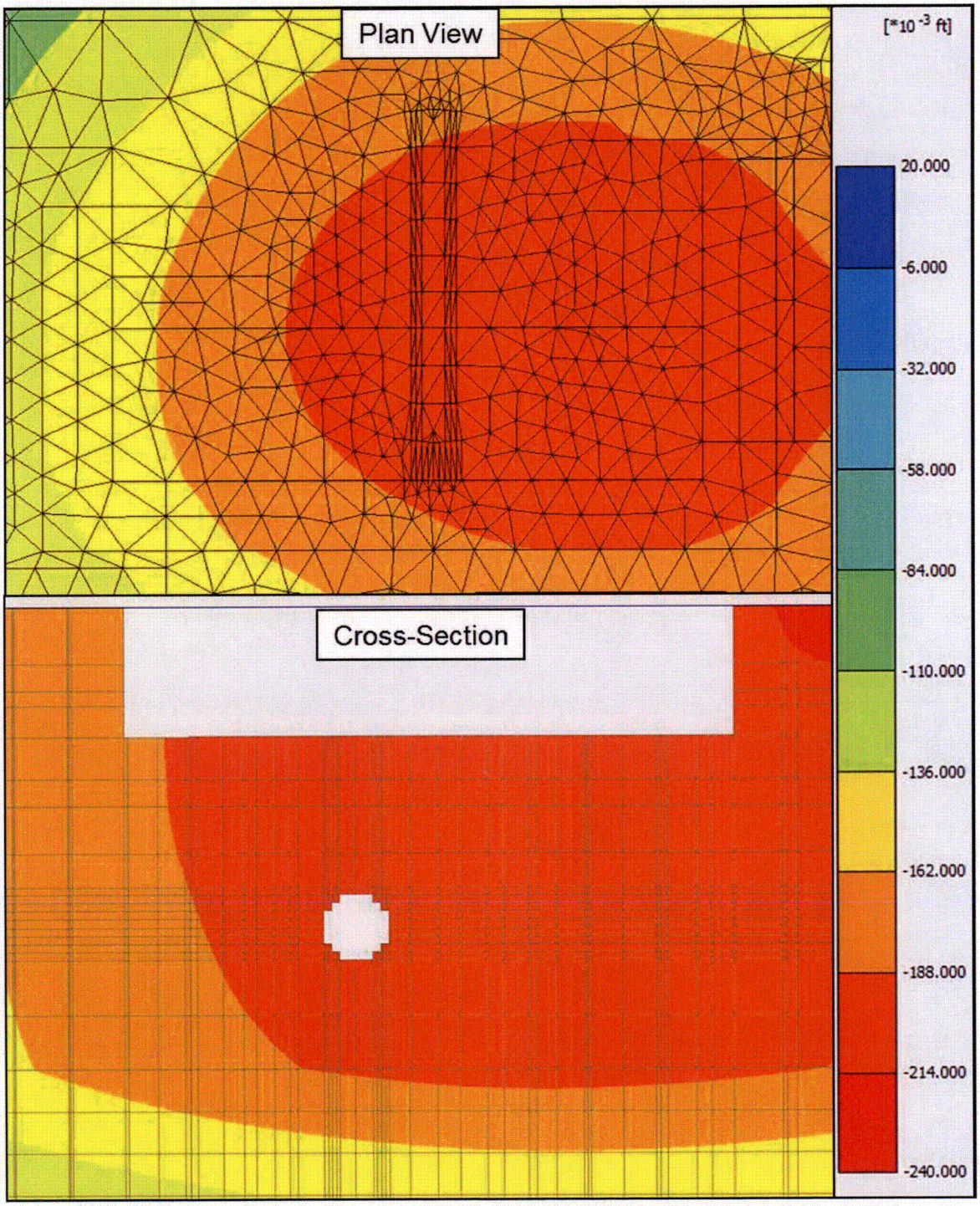

To evaluate bearing capacity, the nuclear island load was incrementally increased and a load displacement curve was developed, as shown in Figure 14. Figure 14 also shows ultimate static and dynamic bearing capacities required by the DCD for factors of safety of 3 and 2, respectively. The required ultimate static and dynamic bearing capacities from the DCD are within the linear elastic range of the load displacement curve. Actual bearing capacity as defined by the load-displacement curve shown in Figure 14 is much higher than DCD limits. The load-displacement curve indicates that the significant reduction in stiffness, which can be defined as the ultimate bearing capacity, does not occur for loads up to 250 ksf, i.e., the actual bearing capacity according to Figure 14 is higher than 250 ksf. Please note the bearing capacity definition used here is not a serviceability limit and is rather an ultimate state, thus, the deformation levels are not relevant in this analysis.

Figure 14 Load Displacement Curve

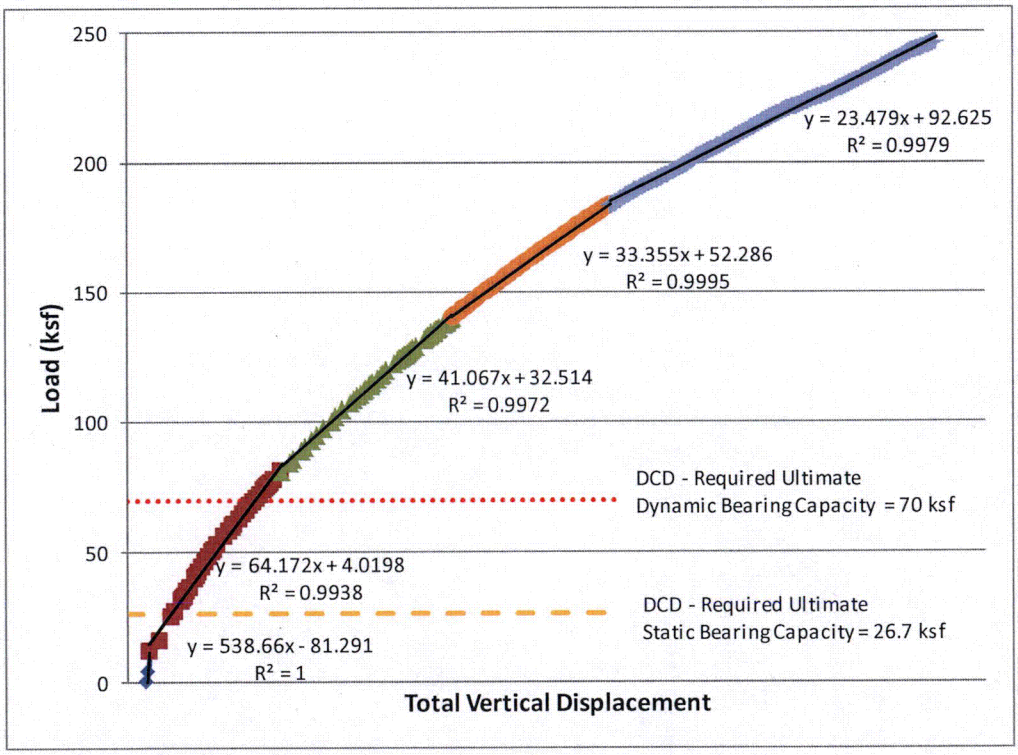

As indicated by the results shown in Figures 11 through 14 and in Table 3:

- No plastic points or tension cut-off points are observed during the loading phase (1x bearing demand),
- The factor of safety for bearing capacity is greater than 3,
- The DCD criteria for settlement are met, and
- The tensile capacity of the concrete fill is not reached.

In summary, the void size constrained by the grouting program has been demonstrated to not be critical to the static stability of safety related structures.

Response under Dynamic Loads

As shown in Figure 15, under pseudo-dynamic loading (multiplier of 1) there are no plastic points (indicated by red squares) or tension cut-off points (indicated by blue squares) near the void location indicating that the rock mass surrounding the void is not experiencing Mohr-Coulomb or points where the tensile load exceeds the tensile capacity. No tension cut-off points are identified in the concrete fill, i.e., the tension in the concrete fill is less than the tensile capacity of the concrete fill.

Figure 15 Plastic Points PLAXIS3D
(Pseudo-Dynamic Loading, Multiplier of 1 as defined in Table 2)

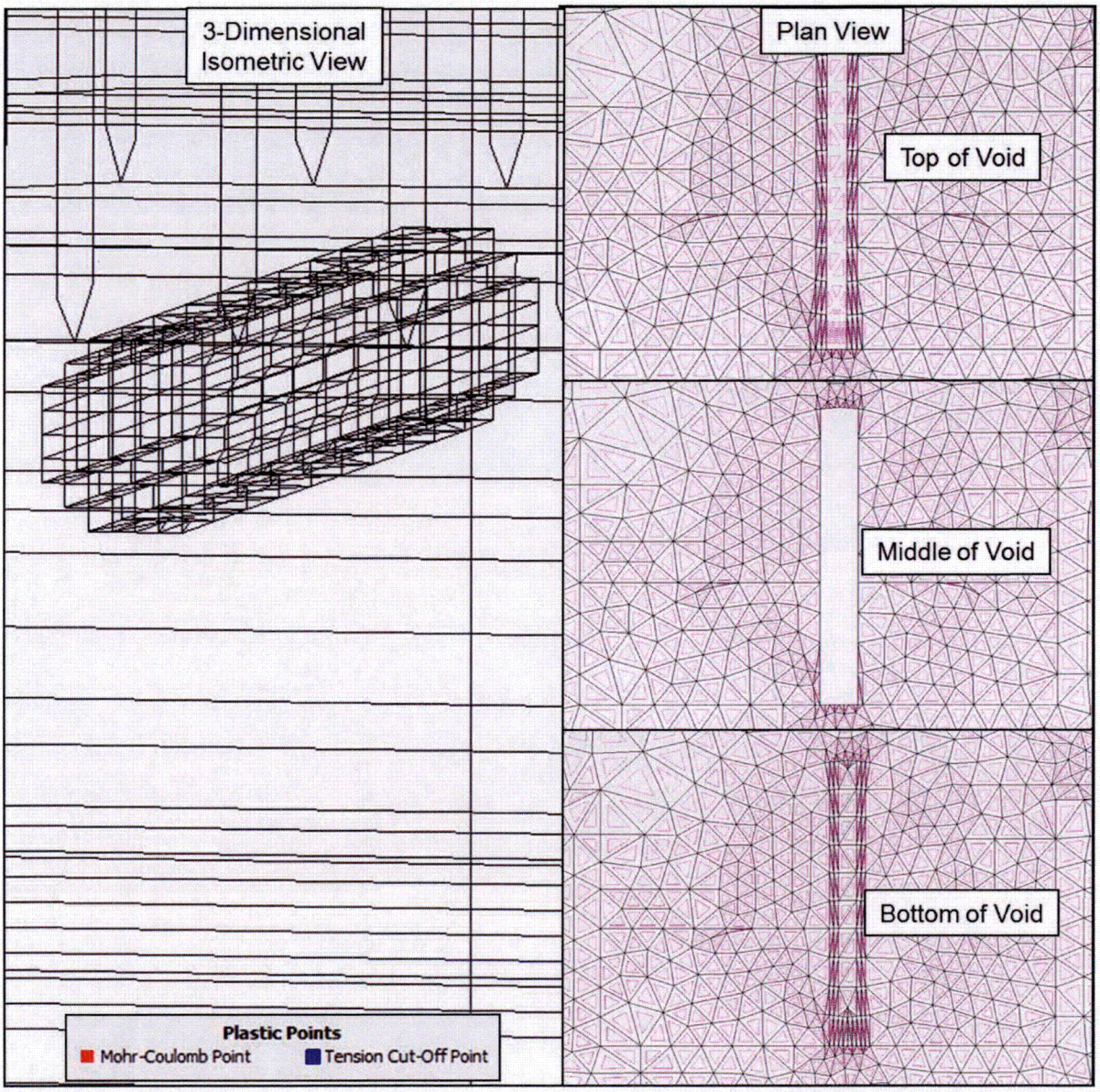

Effective vertical stresses for pseudo-dynamic loading (multiplier of 1) are shown for the concrete fill in Figure 16. The maximum compressive stresses are provided in Table 4 and are much less than the ultimate bearing capacity of the concrete. The maximum compressive stresses provided in Table 4 conservatively represent local maximums for one element and one node only; these stresses are not averaged over multiple elements to distribute the stresses.

Figure 16 Effective Vertical Stresses on Concrete Fill (Pseudo-Dynamic Loading, Multiplier of 1 as defined in Table 2)

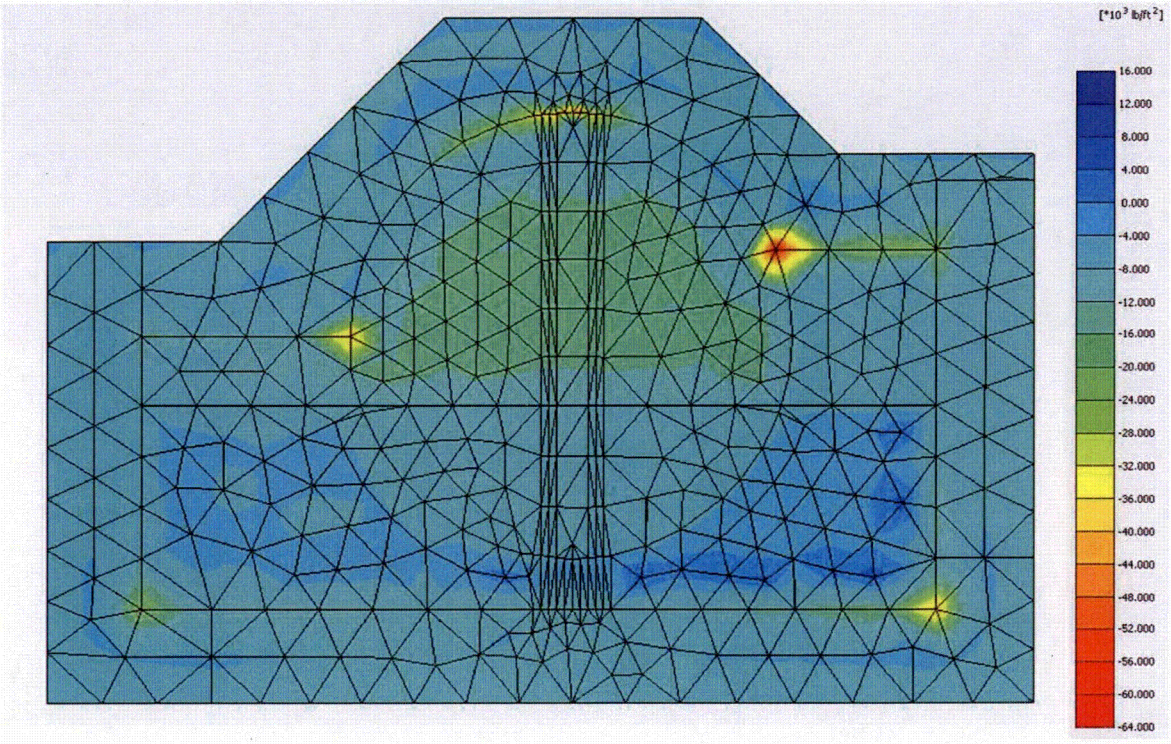

Note: Negative effective stresses represent compression, while positive effective stresses represent tension.

As shown in Figure 17, under pseudo-dynamic loading (multiplier of 2) there are no plastic points (indicated by red squares) or tension cut-off points (indicated by blue squares) near the void location indicating that the rock mass surrounding the void is not experiencing Mohr-Coulomb or points where the tensile load exceeds the tensile capacity. No tension cut-off points are identified in the concrete fill, i.e., the tension in the concrete fill is less than the tensile capacity of the concrete fill.

Figure 17 Plastic Points PLAXIS3D
(Pseudo-Dynamic Loading, Multiplier of 2 as defined in Table 2)

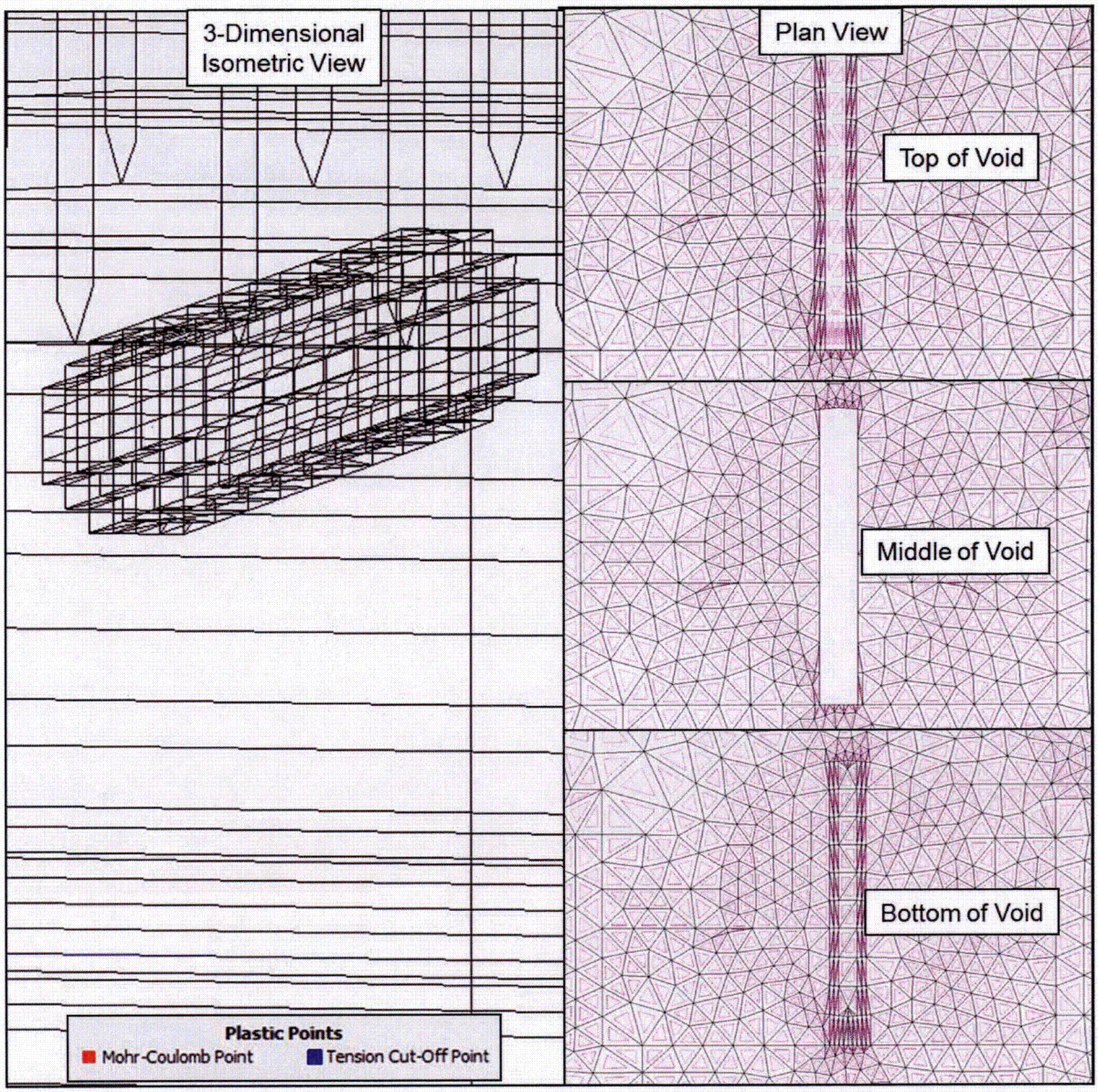

Effective vertical stresses for pseudo-dynamic loading (multiplier of 2) are shown for the concrete fill in Figure 18. The maximum compressive stresses are provided in Table 4 and are much less than the ultimate bearing capacity of the concrete. The maximum compressive stresses provided in Table 4 conservatively represent local maximums for one element and one node only; these stresses are not averaged over multiple elements to distribute the stresses.

Figure 18 Effective Vertical Stresses on Concrete Fill (Pseudo-Dynamic Loading, Multiplier of 2 as defined in Table 2)

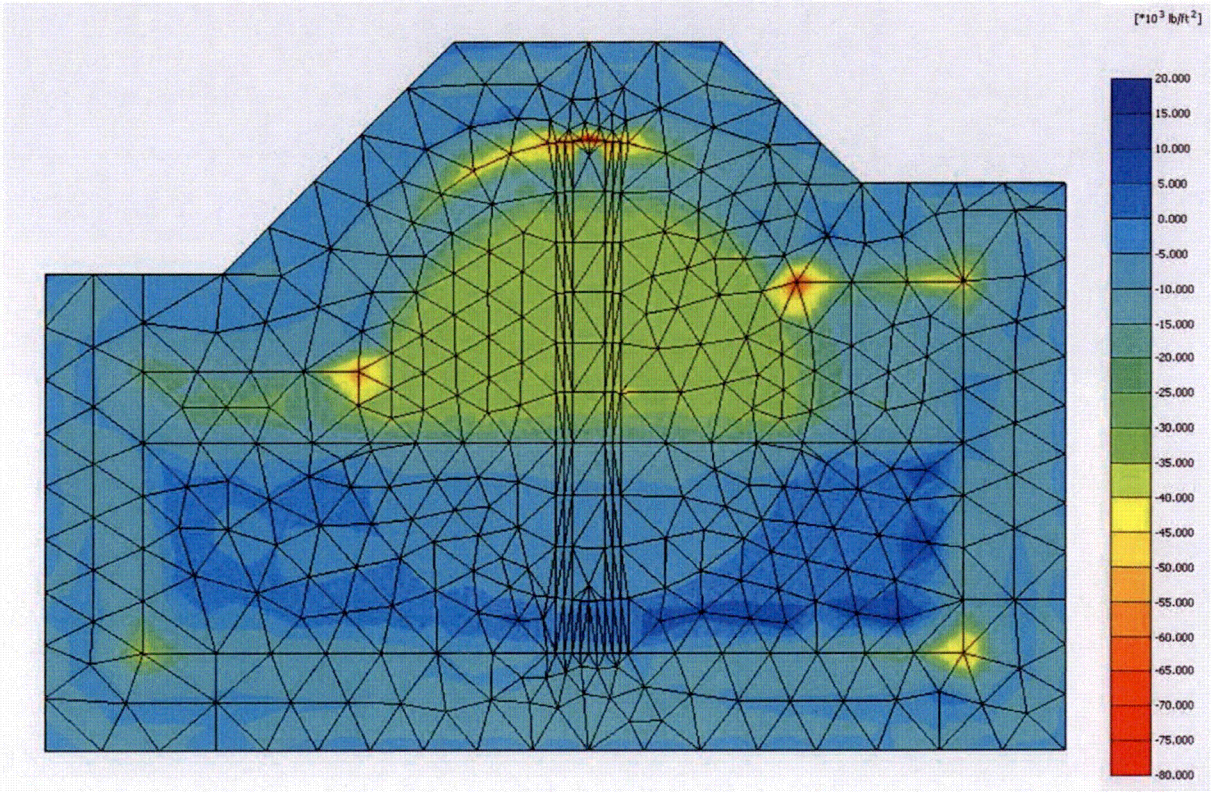

Note: Negative effective stresses represent compression, while positive effective stresses represent tension.

Table 4
Effective Vertical Stress on Concrete Fill (Pseudo-Dynamic Loading)

Pseudo-Dynamic Loading Condition	Maximum Compressive Stress (ksf)	Ultimate Bearing Capacity of Concrete (ksf)
Multiplier of 1	61	184
Multiplier of 2	77	

As indicated by the results shown in Figures 15 through 18 and in Table 4:

- No plastic points or tension cut-off points are observed during the pseudo-dynamic loading conditions,
- The effective vertical compressive stresses are smaller than the ultimate bearing capacity of the concrete, and
- The tensile capacity of the concrete fill is not reached.

In summary, the void size constrained by the grouting program has been demonstrated to not be critical to the pseudo-dynamic stability of safety related structures. In other words, subsurface collapse is not anticipated under the combination of seismic and static Nuclear Island loads.

Part 2)

As discussed in Part 1 of this response, the void size constrained by the grouting program has been evaluated and is not critical to safety related structures. Therefore, any voids smaller than those constrained by the grouting program are also not critical to safety related structures.

Part 3)

As discussed in Part 1 of this response, microgravity methods can only detect large voids at depth. Therefore, the grouting program will be utilized to constrain the void sizes. Within the diaphragm wall, primary and secondary grout boreholes will be drilled and pressure grouted between El. –35 feet and El. –60 feet, and the grout closure criteria will be met. Therefore, any potential voids within this zone are filled. Further, primary grout boreholes will be drilled and pressure grouted down to El. –110, therefore constraining the size of potential voids to 20 feet.

Part 4)

Table 5, below, provides the ITAAC to ensure that any potential voids in the zone between El. –35 feet and El. –60 feet are grouted and that the maximum equivalent spherical diameter of potential voids between El. –60 feet and El. –110 feet are constrained to 20 feet by the grout program.

Table 5
ITAAC for Category I Structure Foundation Grouting (1)

Design Commitment	Inspections, Tests, Analyses	Acceptance Criteria
Any potential voids between El. –35 ± 2 feet and El. –60 ± 2 feet inside the region defined by the diaphragm walls are grouted. The maximum equivalent spherical diameter of potential voids between El. –60 ± 2 feet and El. –110 ± 2 feet is less than 20 ± 2 feet inside the region defined by the diaphragm walls.	1) Grout closure criteria for the grouted zone (between El. -35 ± 2 feet and El. -60 ± 2 feet) are defined in the grout test program. Inside the region defined by the diaphragm walls, drilling and pressure grouting are performed per grout program specifications established as part of grout test program for: (i) Primary and secondary grout boreholes between El. –35 ± 2 feet and El. –60 ± 2 feet (if necessary tertiary and quaternary per closure criteria), and (ii) Primary grout boreholes down to El. –110 ± 2 feet. 2) An as-built survey will be performed to confirm the spacing of grout boreholes.	1) Primary and secondary grout boreholes are drilled and pressure grouted between El. –35 ± 2 feet and El. –60 ± 2 feet. Grout closure criteria for the grouted zone are met as defined in the grout test program. 2) The as-built survey of the grout layout a) Confirms that spacing of primary grout boreholes is less than or equal to 20 ± 2 feet on center. b) Confirms that secondary grout boreholes are offset from primary grout boreholes such that a secondary grout borehole is at the center of the square formed by four adjacent primary grout boreholes. c) Confirms the spacing of tertiary and quaternary grout boreholes if these are necessary per closure criteria.

Note:

(1) All elevations are presented in the North American Vertical Datum of 1988 (NAVD88).

REFERENCES:

1. Bowles, J., *Foundation Analysis and Design*, 5th ed., McGraw-Hill Companies, Inc., New York, 1997.
2. McCormac, J., Nelson, J., *Design of Reinforced Concrete*, Seventh Edition, John Wiley & Sons, Inc., 2006.
3. American Concrete Institute, *Building Code Requirements for Structural Concrete and Commentary*, ACI 318-11, 2011.
4. Brinkgreve, R.B.J. and Swolfs, W.M., *PLAXIS 3D Foundation Version 2 Part 2: Reference Manual*, PLAXIS bv, 2007.

ASSOCIATED COLA REVISIONS:

FSAR Subsection 2.5.4.4.5.5 will be revised in a future COLA revision as follows:

2.5.4.4.5.5 Summary and Commitment

Based on geophysical site characterization data (References 286 and 320)**, and drilling observations as outlined in Subsection 2.5.4.1.2.1,** there is no apparent indication that sinkhole hazards exist at the site. There is also no apparent evidence for the presence of underground openings within the survey area that could result in surface collapse. Large low gravity anomalies with magnitudes less than –30 µGals are only detected outside the power block areas, primarily in areas associated with surface depressions containing vegetation. Once the effects of variations in muck thickness are removed from the residual gravity data, all the remaining low gravity anomalies can be explained by density variations within the Miami Limestone. The results of the drilling program and borehole geophysical data (Subsections 2.5.1.2.4 and 2.5.4.1.2.1) indicate the existence of two preferential secondary porosity flow zones. The extent of rod drops integrated with the field geophysical data supports the interpretation that large voids are absent beneath the footprints of the Units 6 & 7 nuclear islands.

However, considering the uncertainties related to resolution in the geophysical data at depth and away from survey lines, **the subsurface grouting program will be considered in the determination of constrained void sizes. The zone between El. –35 feet and El. –60 feet within the diaphragm walls will be grouted according to the closure criteria that will be developed as part of the grout test program (determined from the results of water pressure tests, evaluation of available boring data, and the target residual permeability of the grouted zone). This grouting will ensure that any potential voids in this zone are filled. In addition, for the zone between El. –60 feet and El. –110 feet within the diaphragm walls, grouting will be performed in every primary grout borehole. Primary grout holes will be spaced less than or equal to 20 feet on center (Figure 2CC-239). This configuration is expected to constrain the maximum undetected void size to approximately 20 feet.** ~~a microgravity survey will be performed on the excavation surface to detect the presence, or verify the absence, of potential water-filled dissolution features beneath the power block. The microgravity survey will be designed to detect 25-foot diameter spherical voids and cylindrical voids as small as 12 feet in diameter at~~

~~the base of the 25-foot-thick grout plug at an elevation of approximately -60 feet NAVD 88. If present, microgravity anomalies may be further investigated by drilling and sampling to determine their origin.~~

FSAR Subsection 2.5.4.10.8 will be added in a future COLA revision as follows:

2.5.4.10.8 Stability of Category I Structures Considering Postulated Voids in Subsurface

Although large voids and karst features are not considered likely at the site, as described in Appendix 2.5AA, a sensitivity analysis is performed to consider stability of Category I Structures with postulated voids in the subsurface.

As discussed in Subsection 2.5.4.4.5.5, the grouting program will be utilized to constrain void sizes. The zone between El. –35 feet and El. –60 feet within the diaphragm walls will be grouted using a multi-stage grouting program; this will ensure that any potential voids in this zone are grouted. For the zone between El. –60 feet and El.–110 feet within the diaphragm walls, grouting will be conducted in every primary grout borehole, constraining the maximum undetected void size to approximately 20 feet.

The void size (20-feet) constrained by the grouting program is conservatively much larger than the estimated void sizes present on site, and is evaluated in the static (settlement and bearing capacity) and dynamic (pseudo-dynamic) analyses.

A very extreme case of a tunnel (cylindrical) shaped void with a 20-foot diameter circular cross-section is considered where the void extends east-west across the nuclear island with the top of the void just below the grout plug (El. –60 feet). This direction is selected since the maximum seismic overturning moment acts in the east-west direction.

The sensitivity analysis considers extremely unlikely and conservative cases that are only reported to show the safety margin provided by the rock mass; these cases are highly unlikely and are not for design purposes.

For the analysis, the 3D finite element model (as presented in Subsection 2.5.4.10.3.2) is updated for the void case presented above. Best estimate material properties (FD1 properties for rock layers) are used for this analysis, as described in Subsection 2.5.4.10.3.

The void is assumed to be water-filled, and is therefore modeled with the same pore pressures as the surrounding rock.

The model considers a construction sequence that includes the following activities:

- **Initial gravity loading (without the void),**
- **Gravity loading (with the void),**
- **Dewatering,**

- **Excavation and fill placement,**
- **Loading, and**
- **Rewatering.**

The void is not considered in the initial gravity loading phase because it would have developed over time; further, inserting the void in the second phase allows for an evaluation of any points reaching Mohr-Coulomb failure due to the presence of the void independent from the other construction activities.

Figure 2.5.4-273 shows the PLAXIS3D model. The 3D mesh is refined to the extent possible in the area surrounding the void. The total number of elements is 103,136.

Settlement

Vertical deformation due to loading is evaluated in the PLAXIS3D finite element models to determine the impact of the potential void on the settlement of the nuclear island. Differential settlements are calculated and the results are compared to the DCD requirements.

Bearing Capacity

To determine the impact of the potential void on the bearing capacity, the model is incrementally loaded up to much higher loads than the actual building loads and a load displacement curve is developed. This curve is used to evaluate the bearing capacity.

Concrete Fill Properties

In order to assess potential tension in the concrete, the concrete is assumed to be a Mohr-Coulomb material in the PLAXIS3D model with a friction angle of 0 degrees, cohesion of 108,000 psf, and tensile strength of 21,600 psf, based on Equation 2.5.4-32 (Reference 217), Equation 2.5.4-33 (Reference 325), and a compressive strength of 1500 psi.

$$Cohesion = \frac{Compressive\ Strength}{2} \qquad \text{Equation 2.5.4-32}$$

$$Tensile\ Strength \approx 0.1 \times Compressive\ Strength \qquad \text{Equation 2.5.4-33}$$

Pseudo-Dynamic

To consider the impact of the potential voids under dynamic conditions, dynamic bearing pressures from the SASSI model are converted to equivalent (approximately) static loads and applied to the PLAXIS 3D model.

The forces from the dynamic bearing pressures are summed up and distributed uniformly over areas of the eastern (maximum uplift) and western half (maximum compression) of the nuclear island. The maximum uplift bearing pressures as obtained from the upper bound, lower bound, and best estimate cases are applied on the east half of the nuclear island, whereas the maximum compressive bearing

pressures as obtained from the upper bound, lower bound, and best estimate cases are applied on the west half of the nuclear island, such that the maximum overturning moment is applied on the western edge of the nuclear island.

This approach is very conservative because

- Nodal maximum bearing pressures are used regardless of their time step (note that maximum pressures for each node correspond to different time steps, i.e., they do not happen at the same time)
- Maximum compressive pressures and tensile pressures are applied at the same time to maximize the overturning moment

Additionally, a case is considered where the load combinations are multiplied by a safety factor of 2. Table 2.5.4-225 shows the total loads considered (static and pseudo-dynamic). The sum of the static load and the seismic uplift pressure is positive, if the overall pressure is compressive.

The bearing pressures corresponding to the combination of dead loads and the maximum moment are checked against the bearing capacity of the concrete fill. The ultimate bearing capacity for the concrete fill is estimated to be 1275 psi (184 ksf) using Equation 2.5.4-34 (Reference 317) and a compressive strength of 1500 psi.

$$Ultimate\ Bearing\ Capacity = 0.85 \times f'c \qquad \text{Equation 2.5.4-34}$$

Where,

f'c = compressive strength

Results

All model results presented are for the case with a tunnel (cylindrical) shaped void with a 20-foot diameter circular cross-section. The tunnel (cylindrical) shaped void is considered to be more critical than a smaller 20-foot diameter spherical void, or a distribution of spherical voids.

The static stability check is governed by the following four factors:

1. Accumulation of plastic points indicating a local (e.g., around the void) or global (e.g., bearing capacity) failure.
2. Deformations exceeding DCD limits.
3. Concrete layer experiencing tension failure.
4. Bearing capacity with FS<3.

Yield at any point is considered to occur if the stress state reaches the Mohr-Coulomb failure envelope. As shown in Figure 2.5.4-274, there are no plastic points or tension cut-off points near the void location indicating that the rock mass surrounding the void is not experiencing compressive failure according to Mohr-Coulomb failure envelope or points where the tensile load exceeds the tensile capacity. No tension cut-off points are identified within the concrete fill,

i.e., the tension in the concrete fill is less than the tensile capacity of the concrete fill.

Another useful parameter to consider is the relative shear stress, which is a measure to define how close the stress state is to the Mohr-Coulomb failure envelope. Relative shear stresses are defined in Equation 2.5.4-35 (Reference 326).

$$\tau_{rel} = \frac{\tau_{mob}}{\tau_{max}} \qquad \text{Equation 2.5.4-35}$$

Where,

τ_{rel} = relative shear stress,
τ_{mob} = mobilized shear strength (maximum value of shear stress),
τ_{max} = maximum value of shear stress for the case where the Mohr's circle is expanded to touch the Coulomb failure envelope while keeping the center of Mohr's circle constant.

Based on Equation 2.5.4-35, relative shear stresses provide a measure of margin compared to Mohr-Coulomb failure. For example, if the relative shear stress is equal to 1, then that location is marked with a plastic point. If the relative shear stress is much less than 1, the point is not close to the Mohr-Coulomb failure envelope. As shown by Figure 2.5.4-275, the rock surrounding the void indicates relative shear stresses much less than 1.

In conclusion, the presence of a 20-foot wide tunnel as modeled here does not present stability concerns, i.e., no subsurface collapse is anticipated.

The total and differential settlements from the PLAXIS3D model indicate that the presence of the void has no impact on settlement, and that the DCD criteria are still met. The total vertical deformation (loading nuclear island phase) from the PLAXIS3D model is shown in Figure 2.5.4-276. Therefore the void cases considered are not critical to the settlement of safety related structures.

To evaluate bearing capacity, the nuclear island load was incrementally increased and a load displacement curve was developed, as shown in Figure 2.5.4-277. Figure 2.5.4-277 also shows ultimate static and dynamic bearing capacities required by the DCD for factors of safety of 3 and 2, respectively. The required ultimate static and dynamic bearing capacities from the DCD are within the linear elastic range of the load displacement curve. Actual bearing capacity as defined by the load-displacement curve shown in Figure 2.5.4-277 is much higher than DCD limits. The load-displacement curve indicates that the significant reduction in stiffness, which can be defined as the ultimate bearing capacity, does not occur for loads up to 250 ksf, i.e., the actual bearing capacity according to Figure 2.5.4-277 is higher than 250 ksf.

As indicated by the results discussed above and shown in Figures 2.5.4-274 through 2.5.4-277,

- **No plastic points or tension cut-off points are observed during the loading phase (1x bearing demand),**
- **The factor of safety for bearing capacity is greater than 3,**
- **The DCD criteria for settlement are met, and**
- **The tensile capacity of the concrete fill is not reached.**

In summary, the void size constrained by the grouting program has been demonstrated to not be critical to the static stability of safety-related structures.

Response under Dynamic Loads

Under pseudo-dynamic loading (multiplier of 1 and multiplier of 2) there are no plastic points or tension cut-off points near the void location indicating that the rock mass surrounding the void is not experiencing Mohr-Coulomb or points where the tensile load exceeds the tensile capacity. No tension cut-off points are identified in the concrete fill.

Effective vertical stresses for pseudo-dynamic loading (multiplier of 1) are shown for the concrete fill in Figure 2.5.4-278. Effective vertical stresses for pseudo-dynamic loading (multiplier of 2) are shown for the concrete fill in Figure 2.5.4-279. For both cases, the maximum compressive stresses are provided in Table 2.5.4-226 and are much less than the ultimate bearing capacity of the concrete. The maximum compressive stresses provided in Table 2.5.4-226 conservatively represent local maximums for one element and one node only; these stresses are not averaged over multiple elements to distribute the stresses.

As indicated by the results described above and shown in Figures 2.5.4-278 and 2.5.4-279 and in Table 2.5.4-226:

- **No plastic points or tension cut-off points are observed during the pseudo-dynamic loading conditions,**
- **The effective vertical compressive stresses are smaller than the ultimate bearing capacity of the concrete, and**
- **The tensile capacity of the concrete fill is not reached.**

In summary, the void size constrained by the grouting program has been demonstrated to not be critical to the pseudo-dynamic stability of safety related structures. In other words, subsurface collapse is not anticipated under the combination of seismic and static nuclear island loads.

The following references will be added to Subsection 2.5.4.13 in a future revision of the COLA:

325. McCormac, J., Nelson, J., *Design of Reinforced Concrete*, Seventh Edition, John Wiley & Sons, Inc., 2006.

326. Brinkgreve, R.B.J. and Swolfs, W.M., *PLAXIS 3D Foundation Version 2 Part 2: Reference Manual*, PLAXIS bv, 2007.

The following tables will be added to Subsection 2.5.4 in a future revision of the COLA:

Table 2.5.4-225
Pseudo-Dynamic Loads (ksf) Considered in Sensitivity Model with 20-Foot Diameter Cylindrical Void

Building	Multiplier of 1		Multiplier of 2	
	West Half of NI	East Half of NI	West Half of NI	East Half of NI
Shield Building	-16.2	-8.1	-32.3	-4.3
North Auxiliary Building	-9.5	-1.4	-18.9	2.4
South Auxiliary Building	-12.1	-4.0	-24.1	-0.2

Note:

Negative sign indicates compressive loads, positive sign indicates uplift loads.

Table 2.5.4-226
PLAXIS3D Effective Vertical Stress on Concrete Fill for Sensitivity Model with 20-Foot Diameter Cylindrical Void

Pseudo-Dynamic Loading Condition	Maximum Compressive Stress (ksf)	Ultimate Bearing Capacity of Concrete (ksf)
Multiplier of 1	61	184
Multiplier of 2	77	

The following figures will be added to Subsection 2.5.4 in a future revision of the COLA:

Figure 2.5.4-273 PLAXIS3D Sensitivity Model with 20-foot Diameter Cylindrical Void

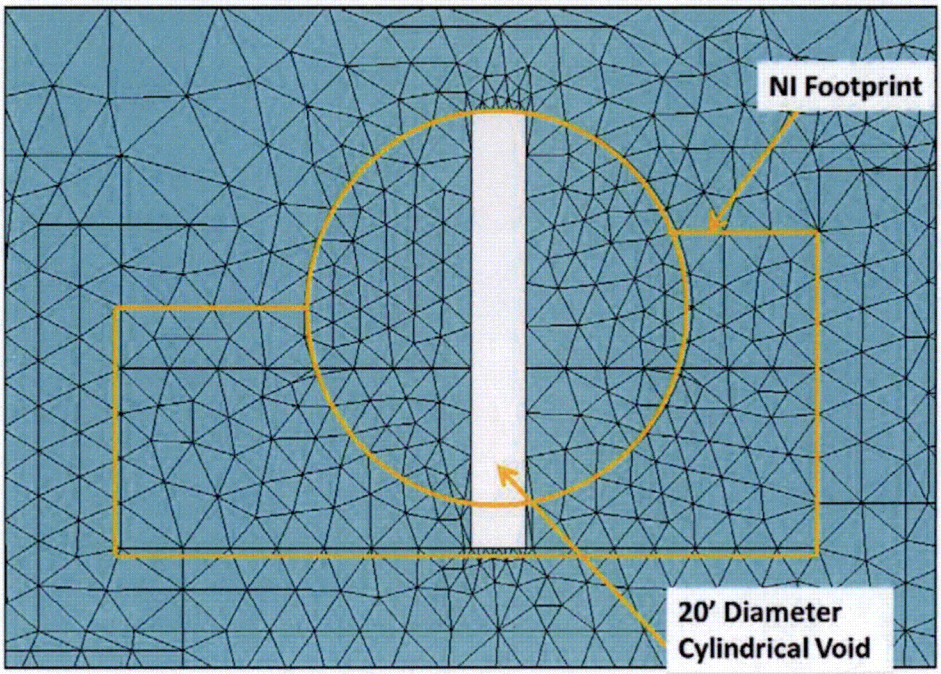

Figure 2.5.4-274 PLAXIS3D Plastic Points for Sensitivity Model with 20-foot Diameter Cylindrical Void (Static Loading)

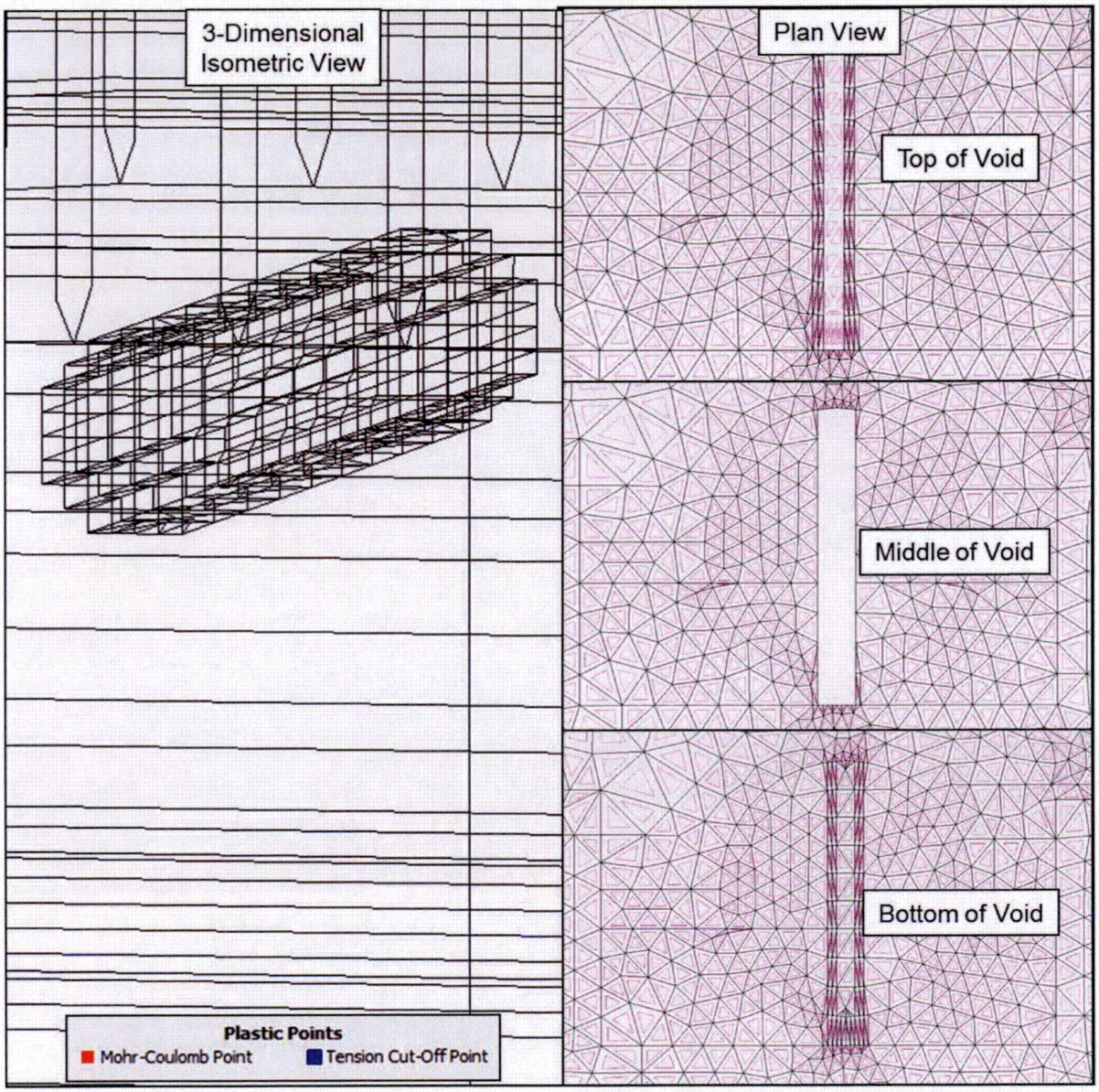

Figure 2.5.4-275 PLAXIS3D Relative Shear Stresses for Sensitivity Model with 20-Foot Diameter Cylindrical Void (Static Loading)

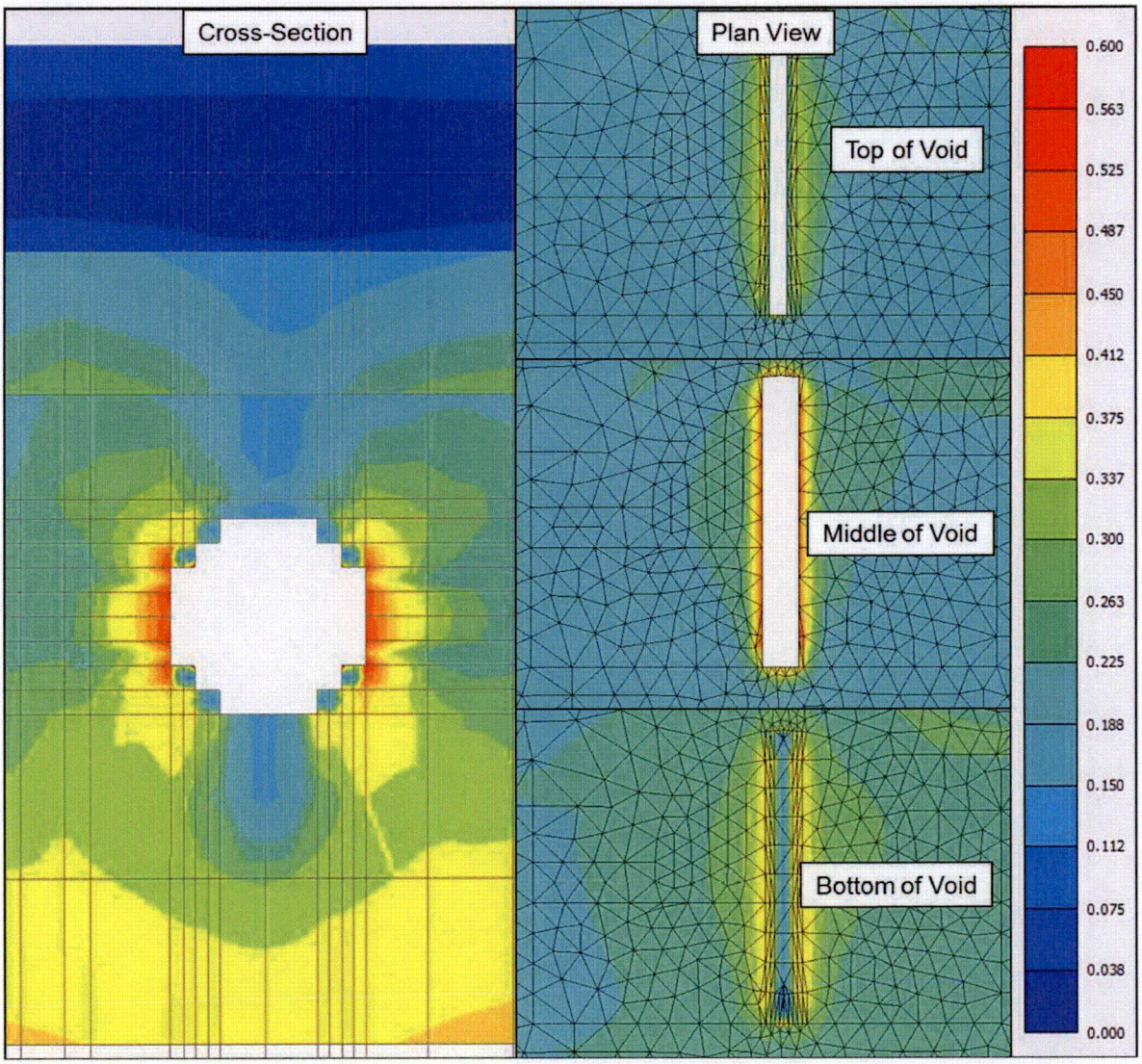

Figure 2.5.4-276 PLAXIS3D Total Vertical Deformation for Sensitivity Model with 20-Foot Diameter Cylindrical Void (Static Loading)

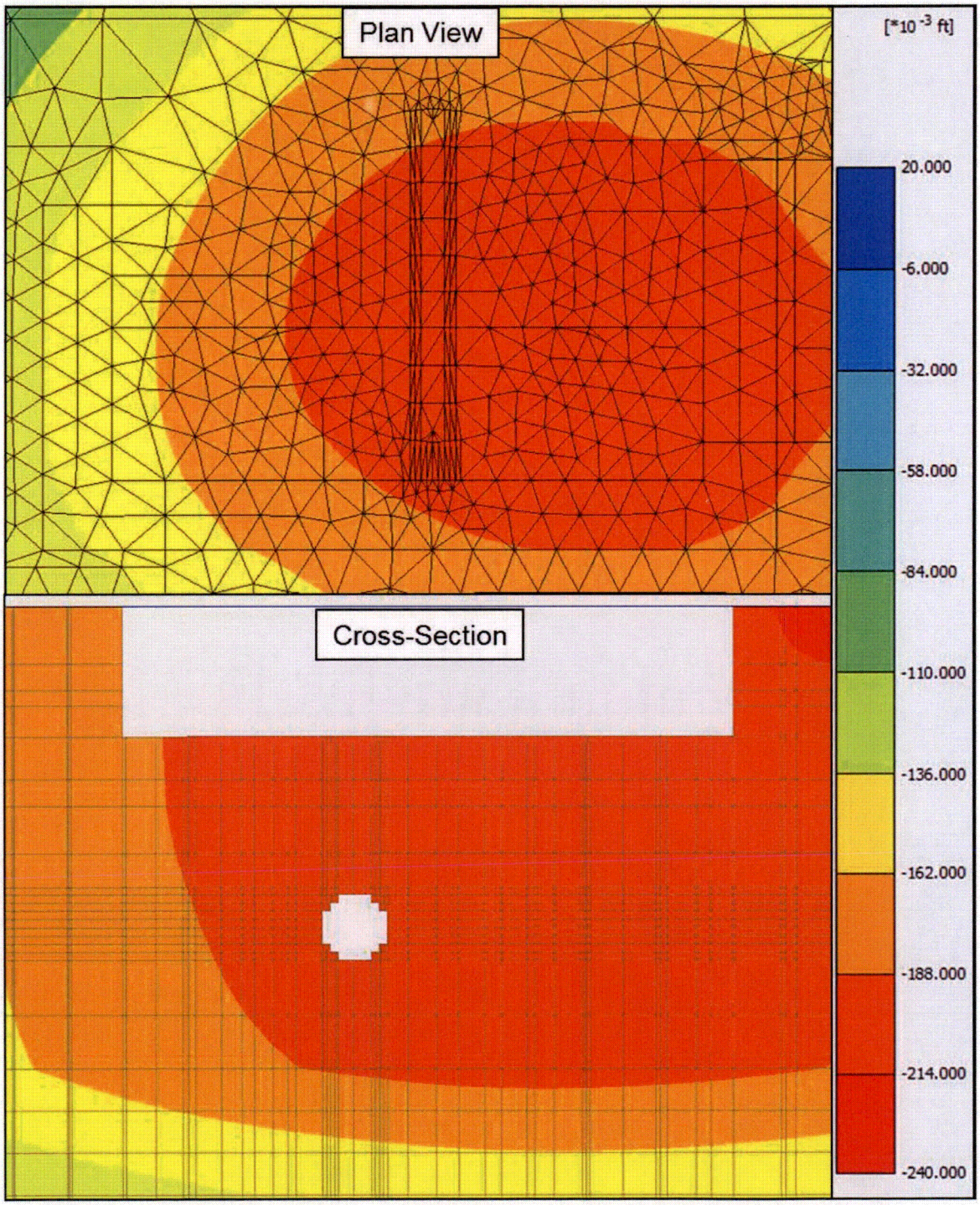

Figure 2.5.4-277 PLAXIS3D Load Displacement Curve for Sensitivity Model with 20-Foot Diameter Cylindrical Void

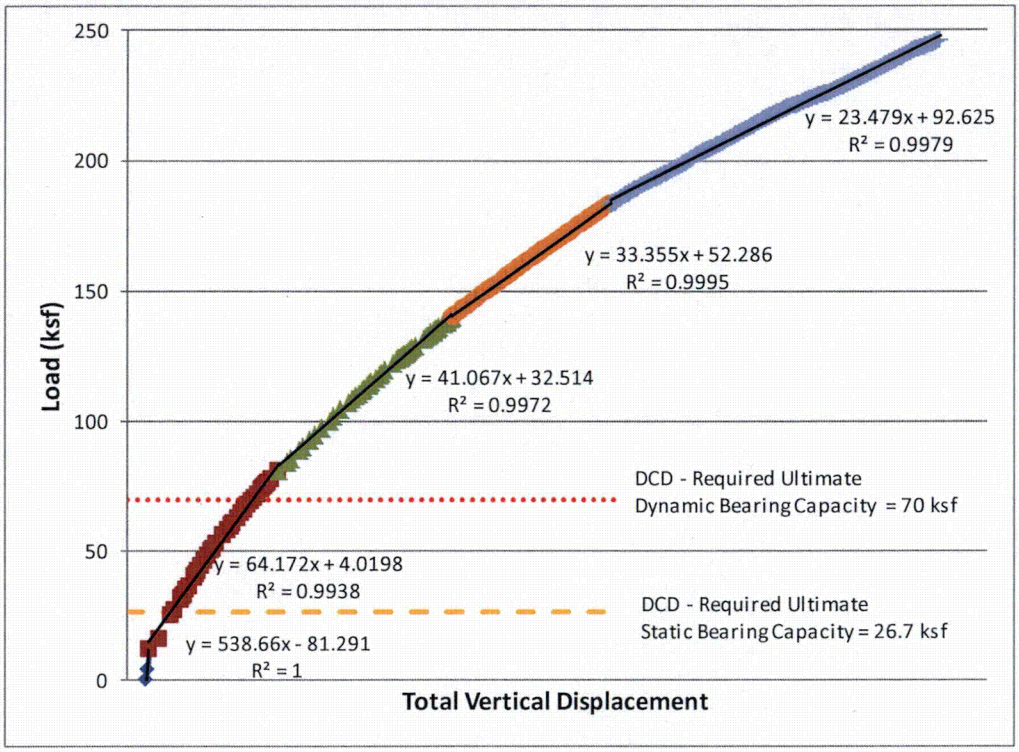

Figure 2.5.4-278 PLAXIS3D Effective Vertical Stresses on Concrete Fill (Pseudo-Dynamic Loading, Multiplier of 1) for Sensitivity Model with 20-Foot Diameter Cylindrical Void

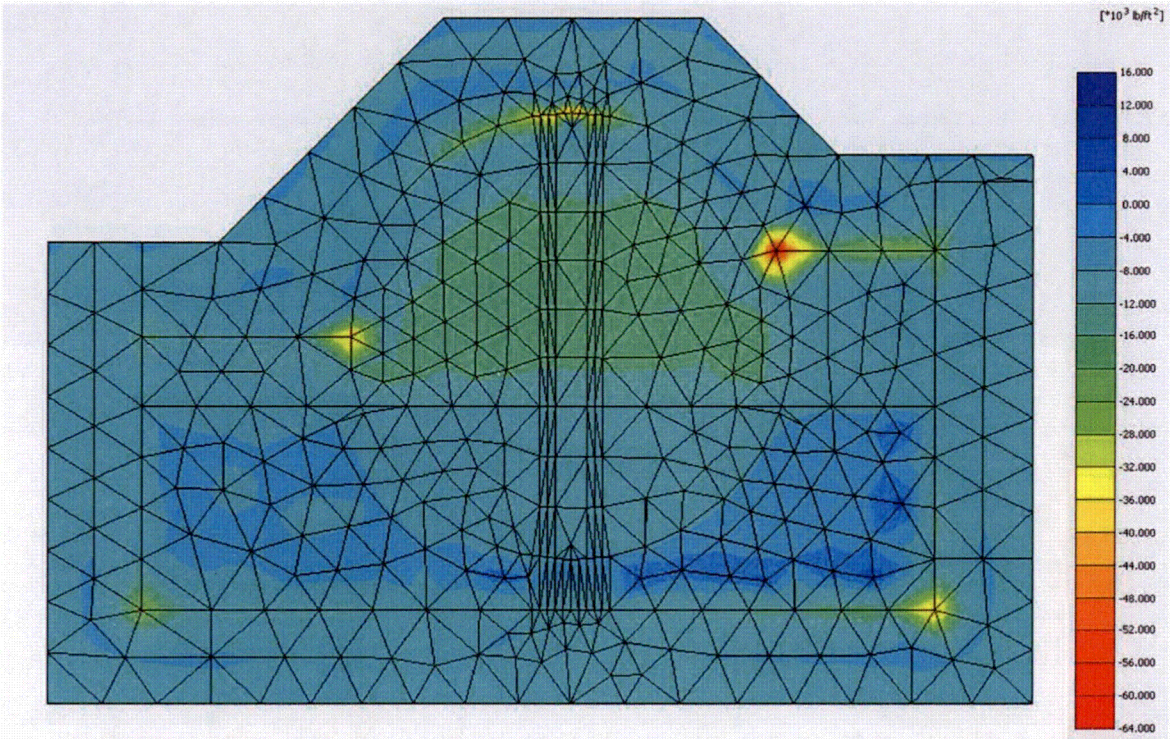

Note: Negative effective stresses represent compression, while positive effective stresses represent tension.

Figure 2.5.4-279 PLAXIS3D Effective Vertical Stresses on Concrete Fill (Pseudo-Dynamic Loading, Multiplier of 2) for Sensitivity Model with 20-Foot Diameter Cylindrical Void

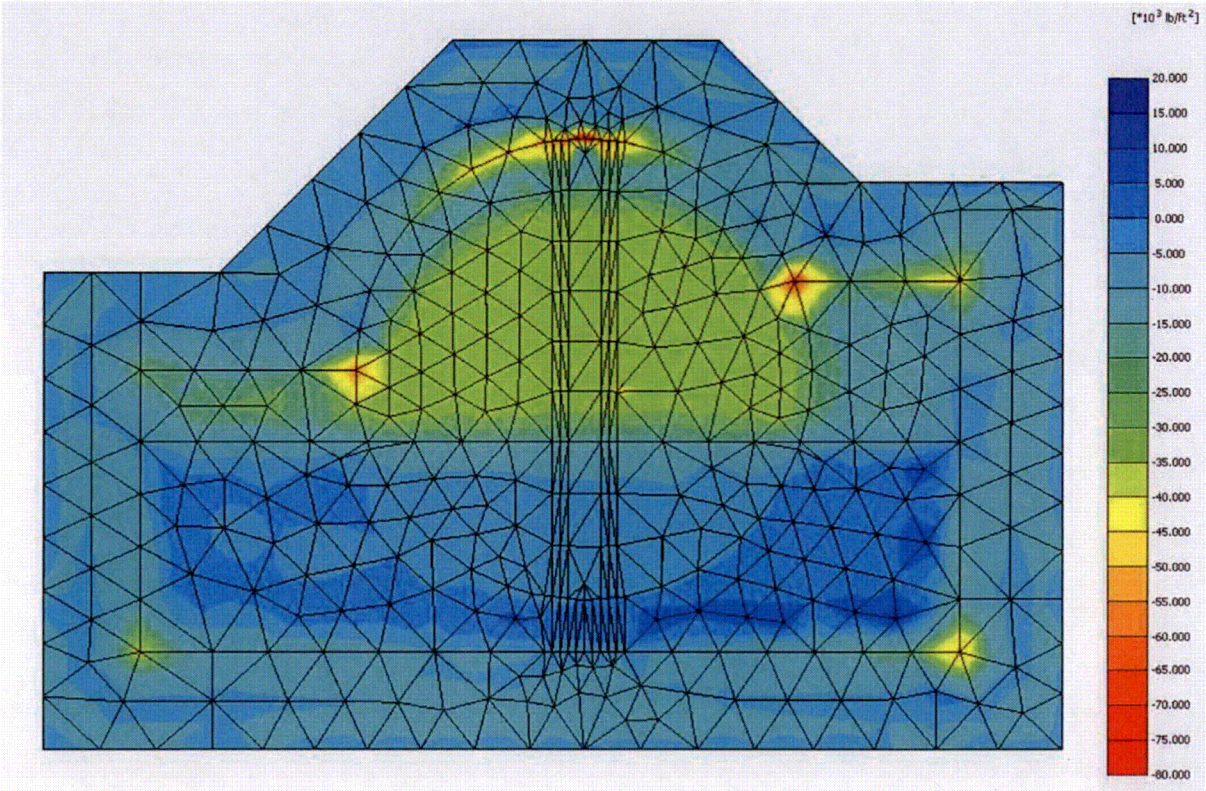

Note: Negative effective stresses represent compression, while positive effective stresses represent tension.

FSAR Subsection 14.3.3.6 will be added in a future COLA revision as follows:

14.3.3.6 ITAAC for Category I Structure Foundation Grouting

This ITAAC ensures that the zone between El. –35 feet and El. –60 feet within the diaphragm walls will be grouted according to the closure criteria that will be developed as part of the grout test program. This grouting will ensure that any potential voids in this zone are filled. In addition, for the zone between El. –60 feet and –110 feet within the diaphragm walls, grouting will be performed in every primary grout borehole. Primary grout holes will be spaced less than or equal to 20 feet on center. This ITAAC ensures that the maximum undetected void size is approximately 20 feet. By verifying that the closure criteria of grout holes are met and the as-built locations of the grout holes, this ITAAC provides a method to confirm that any potential voids between El. –35 feet and El. –60 feet are grouted and that the maximum equivalent spherical diameter of potential voids between El. –60 feet and El. –110 feet is less than 20 ± 2 feet.

The following ITAAC will be added to the COLA, Part 10, Appendix B:

Table 3.8-6
ITAAC for Category I Structure Foundation Grouting (1)

Design Commitment	Inspections, Tests, Analyses	Acceptance Criteria
Any potential voids between El. –35 ± 2 feet and El. –60 ± 2 feet inside the region defined by the diaphragm walls are grouted. The maximum equivalent spherical diameter of potential voids between El. –60 ± 2 feet and El. –110 ± 2 feet is less than 20 ± 2 feet inside the region defined by the diaphragm walls.	1) Grout closure criteria for the grouted zone (between El. –35 ± 2 feet and El. –60 ± 2 feet) are defined in the grout test program. Inside the region defined by the diaphragm walls, drilling and pressure grouting are performed per grout program specifications established as part of grout test program for: (i) Primary and secondary grout boreholes between El. –35 ± 2 feet and El. –60 ± 2 feet (if necessary tertiary and quaternary per closure criteria), and (ii) Primary grout boreholes down to El. –110 ± 2 feet. 2) An as-built survey will be performed to confirm the spacing of grout boreholes.	1) Primary and secondary grout boreholes are drilled and pressure grouted between El. –35 ± 2 feet and El. –60 ± 2 feet. Grout closure criteria for the grouted zone are met as defined in the grout test program. 2) The as-built survey of the grout layout a) Confirms that spacing of primary grout boreholes is less than or equal to 20 ± 2 feet on center. b) Confirms that secondary grout boreholes are offset from primary grout boreholes such that a secondary grout borehole is at the center of the square formed by four adjacent primary grout boreholes. c) Confirms the spacing of tertiary and quaternary grout boreholes if these are necessary per closure criteria.

Note:
(1) All elevations are presented in the North American Vertical Datum of 1988 (NAVD88).

ENCLOSURES:

None

NRC RAI Letter No. PTN-RAI-LTR-082

SRP Section: 02.05.04 - Stability of Subsurface Materials and Foundations

Question from Geosciences and Geotechnical Engineering Branch 1 (RGS1)

NRC RAI Number: 02.05.04-27 (eRAI 7811)

FSAR Subsection 2.5.4.5.4 states that grouting will be conducted beneath the nuclear island between the elevations of approximately -35ft and -60 ft to form a grout plug for construction related groundwater control. In accordance with 10 CFR 100.23 and RG 1.208, please describe what inspection and test programs will be conducted for ensuring the shear wave velocity post grouting is consistent with the shear wave velocity used in the site response analyses you performed in your previous calculation of the GMRS in FSAR Subsection 2.5.2.6.

FPL RESPONSE:

Please note that all elevations referred to in this RAI response are relative to North American Vertical Datum of 1988 [NAVD 88].

As described in FSAR Subsection 2.5.4.6.2, grouting will be performed within the excavation area for the Nuclear Island for construction-related groundwater control. A grout plug is proposed between the bottom of the excavation for the nuclear island (El. –35 feet) and the bottom of the diaphragm wall (El. –60 feet).

The grouted zone (Zone 1) between El. –35 feet and El. –60 feet encompasses approximately 14 feet of the Key Largo Limestone Formation (average top El. –27 feet) and approximately 11 feet of the Fort Thompson Formation (average top El. –49.4 feet). This zone shows the shear wave velocity profiles ranging from approximately 4000 ft/s to 8000 ft/s, as seen on Figures 1 and 2.

As described in the Response to RAI 02.05.04-26, primary grout boreholes will be drilled and pressure grouted between El. –60 feet and –110 feet to constrain the size of postulated voids in the Fort Thompson Formation below Zone 1. The extended zone (Zone 2) between El. –60 feet and –110 feet shows the shear wave velocity profiles ranging from approximately 2500 ft/s to 7000 ft/s, as seen on Figures 1 and 2.

Figure 1 Shear Wave Velocity Profile

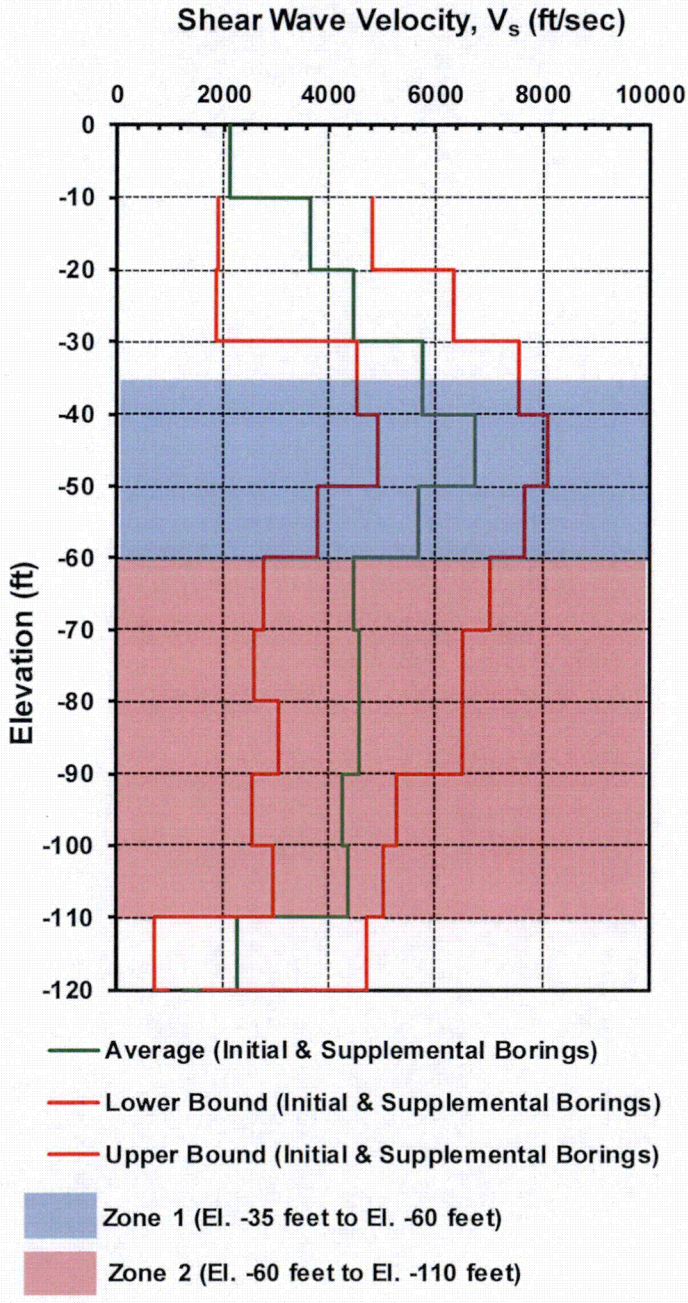

Reference: Data from FSAR Figure 2.5.4-220.

Figure 2 Shear Wave Velocity – All Data

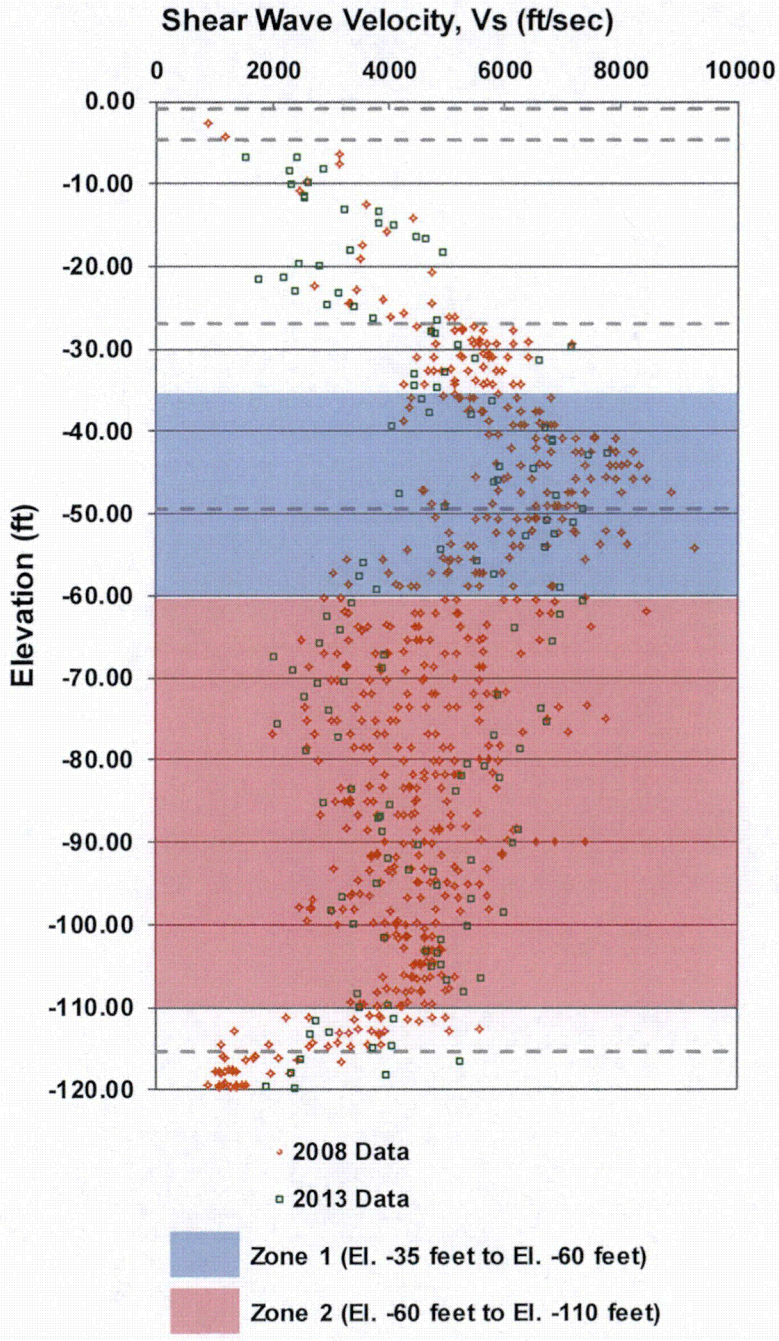

Reference: Data from References 1 and 2.

If there is a change in shear wave velocity due to grouting, it is expected that the post-grouting shear wave velocity would be higher than the pre-grouting shear wave velocity. Further, any increase in shear wave velocity of the Key Largo and Fort Thompson formations is not expected to cause any increase in SSI analysis results, if the input motion remains the same.

A sensitivity analysis was performed to examine the effect of potential increase in shear-wave velocity due to grouting on site amplification. For the purpose of site amplification sensitivity analysis, three dynamic property profiles are considered:

- "Un-grouted" Profile: The BE profile for the NI soil column under un-grouted conditions. This profile serves as the reference case for comparison.
- "Grouted Zone 1" Profile: Same as the "Un-grouted" profile except for Zone 1 (El. –35 to –60 feet), where shear-wave velocity and unit weight for grouted conditions are used, see Table 1.
- "Grouted Zones 1 & 2" Profile: Same as the "Grouted Zone 1" profile except for Zone 2 (El. –60 to –110 feet), where shear-wave velocity and unit weight for grouted conditions are used, see Table 1.

Please note that the "Grouted Zone 1" and "Grouted Zones 1 & 2" profiles include shear wave velocities that are very high. These velocities are not likely to be reached due to grouting, and could be considered as upper bound shear wave velocities.

A comparison of the 5 percent damped acceleration response spectra for the low-frequency motion at the 1E-5 hazard level is presented in Figure 3. While the three profiles result in almost identical site amplification in the low frequency range (below 1 Hz), the "Grouted Zone 1" and "Grouted Zones 1 & 2" cases yield lower site amplification in the higher frequency range. The only exception is around 30 Hz, where the "Grouted Zones 1 & 2" case results in a slight increase in site amplification. Given the large margin between the NI FIRS and the site-specific SSE motion in the high-frequency range, the small increase, observed at 30 Hz in the case of the "Grouted Zones 1 & 2" profile, does not impact the site-specific SSE motion.

Based on the sensitivity analysis results, even if the shear wave velocity significantly increases due to grouting, site-specific SSE motion would still be valid. Therefore, there is no need for an ITAAC to measure the shear-wave velocity of the grouted rock in the field.

Table 1
Shear-Wave Velocity for Zones 1 & 2

Zone	Top Depth[1] (ft)	Top Elevation[1] (ft)	Thickness (ft)	Un-grouted Conditions			Grouted Conditions		
				Unit Weight (kcf)	V_S (ft/sec)	Average V_S (ft/sec)	Unit Weight (kcf)[2]	V_S (ft/sec)	Average V_S (ft/sec)
Zone 1	60.5	-35	6	0.137	5552.5	6075	0.155	7312.2	8000
	66.5	-41	8.4	0.137	6865.2		0.155	9040.8	
	74.9	-49.4	1.6	0.137	6865.2		0.155	9040.8	
	76.5	-51	10	0.137	5738.1		0.155	7556.6	
Zone 2	86.5	-61	10	0.137	4708.4	4504	0.151	5753.7	5504
	96.5	-71	10	0.137	4498.6		0.151	5497.4	
	106.5	-81	10	0.137	4578.9		0.151	5595.5	
	116.5	-91	10	0.137	4284.5		0.151	5235.8	
	126.5	-101	10	0.137	4471.2		0.151	5463.9	

(1) These elevations (and depths), reported in the table and used for site response analysis, are based on P-SHAKE layering, and differ by a 1-foot margin from the nominal elevations (El. –60 feet and El. –110 feet) that correspond to the bottom of Zones 1 and 2, respectively.

(2) The unit weight for grouted conditions in Zone 1 (0.155 kcf) is computed based on the assumption that grout covers 90% of the voids in the rock. The unit weight for grouted conditions in Zone 2 (0.151 kcf) is based on a 10% increase from the unit weight of un-grouted rock (0.137 kcf).

Figure 3 ARS at NI Foundation Horizon Computed using LF 1E-5 Input Motion

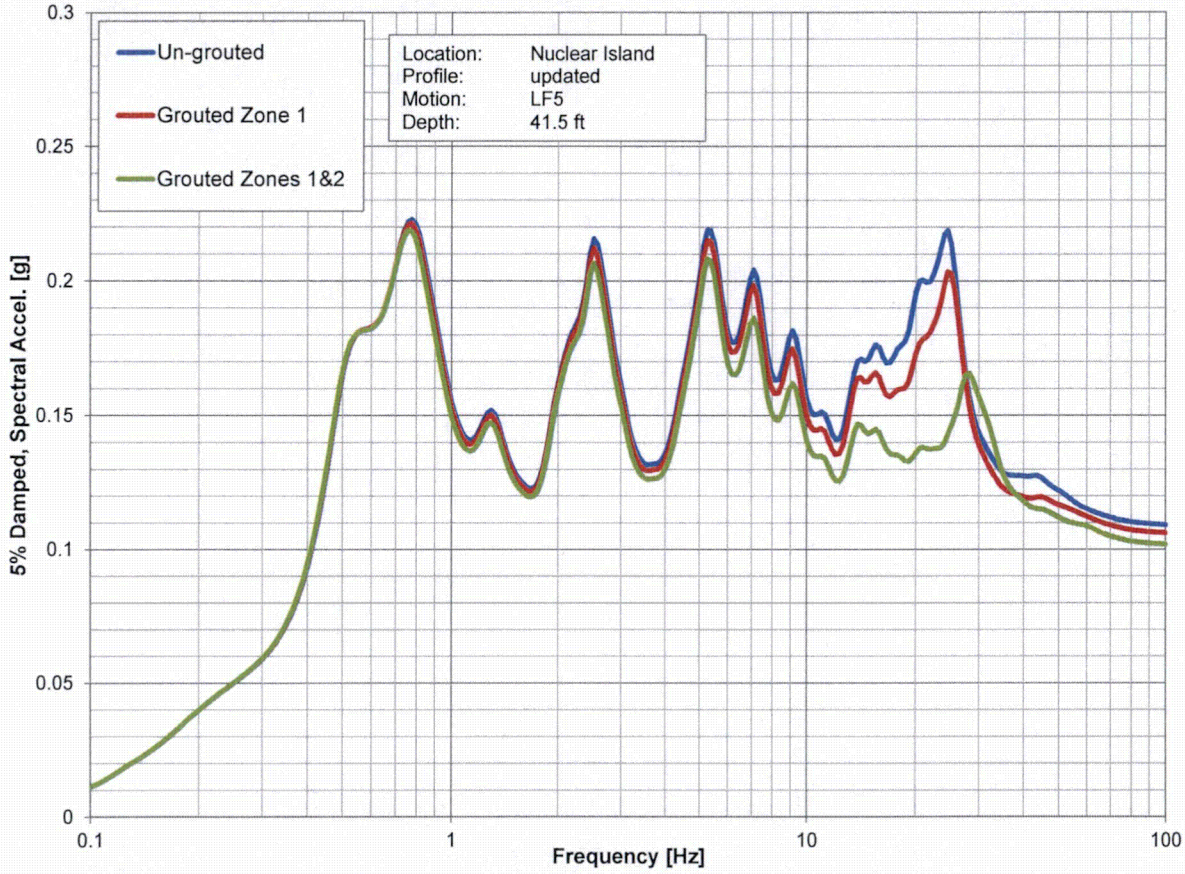

REFERENCES:

1. Paul C. Rizzo Associates, Inc., *Supplemental Field Investigation Data Report, Turkey Point Nuclear Power Plant Units 6 & 7*, Rev. 2, Pittsburgh, Pennsylvania, included In COL Application Part 11, April 15, 2014.

2. MACTEC Engineering and Consulting, Inc., *Final Data Report – Geotechnical Exploration and Testing: Turkey Point COL Project Florida City, Florida*, Revision 2, included in COL Application Part 11, October 6, 2008.

This response is PLANT SPECIFIC.

ASSOCIATED COLA REVISIONS:

None.

ENCLOSURES:

None